SCHOOL OF CIVIL, ENVIRONMENTAL & CHEMICAL ENGINEERING

ENGINEERING CAPSTONE – Part B

Final Report

Novel in-situ fibrous bed bioreactor modelling and microbiome interactions

Tyrone Jonathan Grupel (s3540526)
Tina Gunasekara (s3485773)

10 March, 2023

Academic Supervisors
Dr. Srinivas Mettu
Dr. Namita Choudhury
Dr. Qiang Sun

1. Acknowledgements

Thank you to Dr. Srinivas Mettu and Dr. Qiang Sun for their extensive help with the model and Dr. Namita Choudhary with her assistance with the microbiome interactions.

2. Executive Summary

The bi-directional interactions of the gut microbiome and the drug rosuvastatin was deliberated to analyse its' influences in patients that are at risk of cardiovascular diseases (CVD). As cardiovascular disease is a leading cause of death and affecting an estimated 126 million people worldwide, it is regarded as a threat to sustainable development due to chronic disabilities and impaired quality of life in the western world. Statins are a treatment of choice for patients managing CVD risks, patients with associated CVD and hypercholesterolaemia.

An assessment of patients at risk of CVD undertaking rosuvastatin therapy was selected, where patient grouping was focused on for effective management and understanding of the bi-directional interactions of the microbiome and the statin drug class. The gut microbiome has been associated to numerous drug interactions and is thought to influence the efficacy of pharmacological treatments. Although statins are widely prescribed medications, considerable variability remains in its therapeutic response. We investigated the following bi-directional interactions in:

- The role statins have in gut microbial environment modulation
- The potential influence that the gut microbial composition has on the lipid-lowering efficacy of rosuvastatin

Observations and trends that were analogous was that the genus *Lactobacillus*, falling under the phylum Firmicutes presented better statin response and frequently improved the low-density lipoprotein (LDL) and total cholesterol (TC) levels in patients at risk of CVD. Higher gut biodiversity was also associated with a greater statin response.

Previous research in Semester 1, 2020, has indicated that a hydrogel in-situ fibrous bed bioreactor is a feasible method in gut microbiome simulation. However, due to COVID-19 pandemic, a computational dynamic gut model was produced to mimic the defined growth regions in this microenvironment. Therefore, the bacterial strain *Lactobacillus bulgaricus* was implemented to monitor its modulation on the gut in order to understand the behaviour of bacterial strains and the gut microenvironment. *Lactobacillus bulgaricus* is associated with reducing cholesterol levels in assistance to the statin drug class.

L. Bulgaricus has shown to be an excellent synecdoche for microbiota that display obligative aerobic growth as it is a relatively weak facultative anaerobe. Its oxygen consumption was utilised in a Crank-Nicholson numerical modelling scheme to realistically adjust the level of oxygen concentration in the in-site fibrous bed reactor that has diffused from the atmosphere. It was found that the rate of oxygen diffusion was significantly higher than the net oxygen consumption of the bacteria across lag and logarithmic growth which further adds credence to the model's usability on a lab scale.

The final MATLAB code allows for full customisation of diffusion rates and probiotic oxygen consumption to serve as a sandbox for future research. Quantitatively modelling the growth of bacteria will be useful for modelling gnotobiotic systems and allowing for more conclusive testing of the both the therapeutic and adverse side effects of statins on gut microbiota.

3. Table of Contents

4. List of Figures and Tables

4.1 List of Figures

4.2 List of Tables

5. Introduction

The HMG-CoA reductase inhibitor, commonly known as statins, is a class of drugs that is prescribed extensively to lower total and LDL (low-density lipoprotein) cholesterol levels in the body by manipulating the HMG-CoA (5-hydroxy-3-methylglutaryl-coenzyme A) reductase enzyme, an enzyme required for cholesterol biosynthesis (Zhou & Liao, 2009). Statins are the treatment of choice for patients managing cardiovascular risks and hypercholesterolaemia due to its proven efficacy and safety profile (Schachter, 2005). Rosuvastatin is a newly developed statin that is the most common for patient therapy due to its efficacy.

The human gut microbiome is a diverse and complex ecosystem, comprising of up to 10^{13} – 10^{14} microorganisms (Martin, et al., 2014). The precise compositions of the bacterial communities within the gut microbiota is dependent on environmental factors (dietary habits, drugs and microbial inocula), secretory products, host genotype and peristalsis (Egert, et al., 2006). It has been established that host diet plays a major role in microbial composition. Therefore, an analysis on patients at risk of cardiovascular diseases undertaking rosuvastatin therapy was selected to focus on patient grouping for more effective management and understanding of the bi-directional interactions of the microbiome and rosuvastatin.

Due to the high variability in the composition of gut microbiota within the human population and incomplete data makes it difficult to produce fully deterministic modelling in the human gut microbiome. Further patient classification should be made for accurate prognosis such as diagnosis related groups (DRG), age group, country and sex. However, due to absence of literature available in these specificities, an overview was completed by addressing valuable relationships that may be of help in future research. Computational modelling will play a major role in interpretating experimental data and forecasting responses for dietary modulation. Computational modelling will assist in the simulation of the bi-directional interactions of the statin drug with use of probiotics, in a non-invasive manner that will prove higher accuracy and be more valuable in gaining a comprehensive understanding than in-vitro studies that are available.

6. Statin Review

6.1 Epidemiology of cardiovascular disease

Cardiovascular disease is the collective name for diseases including coronary heart disease (CHD), acute coronary syndrome (ACS) and coronary artery disease (CAD) among other conditions. Coronary heart disease may result in coronary artery disease, whilst acute coronary syndrome is regarded as a subcategory of CAD. Coronary artery disease is characterised by the presence of atherosclerosis in the arterial wall and typically asymptomatic, whereas acute coronary syndrome has a symptom of unstable angina and correlated with myocardial infarction (MI). Mortality due to coronary artery disease is resultant of coronary heart disease (Sanchis-Gomar, et al., 2016).

Cardiovascular diseases are the cause of nearly one-thirds of deaths worldwide in people older than 35 years and is a key cause of death and disability in the western world. While the mortality of CHD has declined in the past decades, it is still acknowledged as a crucial threat to sustainable development due to chronic disabilities and an impaired quality of life. Although cardiovascular disease is preventable, poor nutrition due to industrial culture, nicotine abuse and physical inactivity have increased its incidence in some countries. Increased rates of global population aging in the past two decades will additionally increase the prevalence of CHD, with United Nations reporting a population age of 1 in 11 who are over 65 years old, and estimates an increase to 1 in 6 by 2050 (Our World Data, 2016). Further, due to globalisation and rapid urbanisation in low and middle-income countries (LMIC), a shift from disease-related mortality and impairment from infectious diseases to non-communicable diseases like CHD can be observed.

The American Heart Association has reported that 15.5 million people over the age had CHD in the United States, with an increase in prevalence for both men and women. Death rate due to CHD had significantly decreased from 39% to 23% in comparison with 2003 and 2013, respectively (Sanchis-Gomar, et al., 2016). Absolute numbers of CVD mortality have shown significant growth since 1990, but in this same period, a decrease by 22% in age-standardised death rate was also noted. This is markedly due to a shift in the aging population and diverse causes of death worldwide. The World Health Organization reported in a compiled study of 49 countries including northern Asia and Europe, that 4 million annual deaths had been reported due to cardiovascular diseases (Nichols, et al., 2014). In China, higher risks of CHD had been reported with increased mortality rates in Beijing, accrediting to higher cholesterol levels predominant in the population (Nichols, et al., 2014). In addition, studies have shown that the lifetime risk of developing coronary heart disease in the United States with more than 2 major risk factors present is 18.3% for women and 37.5% for men (Sanchis-Gomar, et al., 2016).

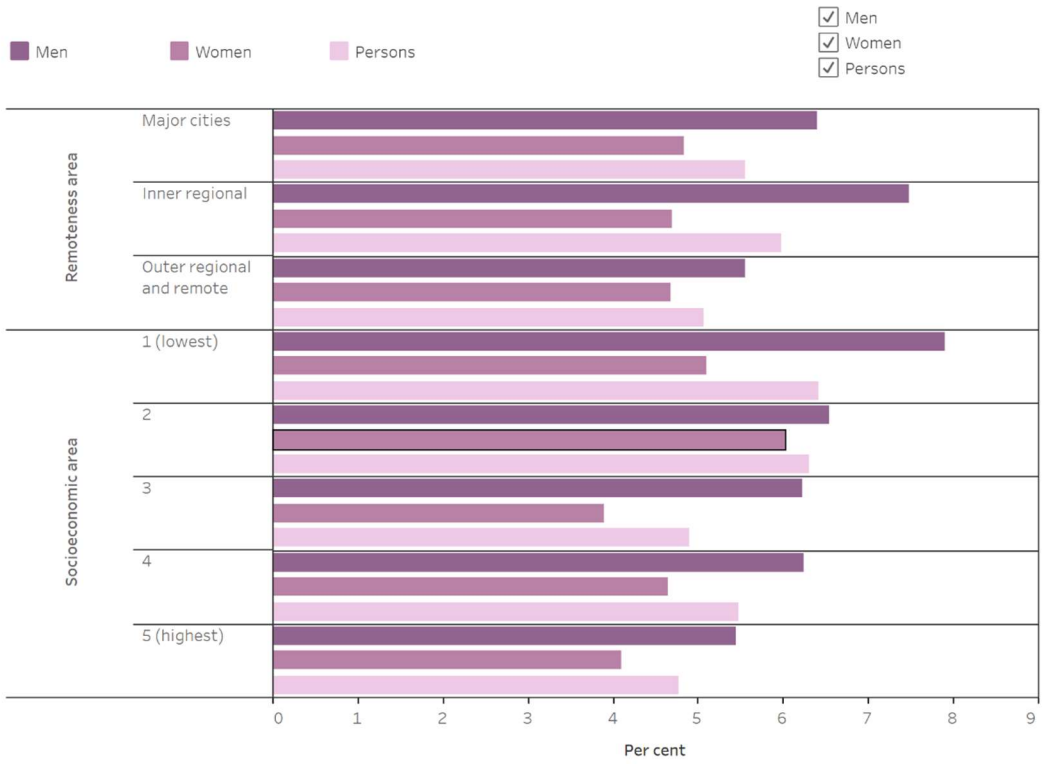

Figure 1. Prevalence in vascular related diseases (CVD, heart and stroke) over the age of 18 (Australian Institute of Health and Welfare, 2020)

The Australian Institute of Health and Welfare estimated that 1.2 million (5.6%) Australians aged over 18 years was reported with one or more vascular-related diseases (CVD, heart or stroke). Coronary heart disease was estimated in 580,300 (2.8%) Australians aged over 18. The Australian Bureau of Statistics reports that CHD prevalence was lower in women (1.9%) compared to men (3.8%) and increased with age. More than 1 in 4 Australians over the age of 75 was depicted with stroke, heart and vascular-related diseases. Remote areas did not show significant differences in CHD prevalence, but socioeconomically disadvantaged areas showed significant differences when compared with least disadvantaged areas (Australian Institure of Health and Welfare, 2020).

It was estimated that acute coronary events (unstable angina or heart attack) were prevalent in 59,100 persons over the age of 25, with an approximate daily hospitalisation of 162 events. Trends show that the rates of acute coronary events declined by 42% (2007-2017) (Australian Institure of Health and Welfare, 2020).

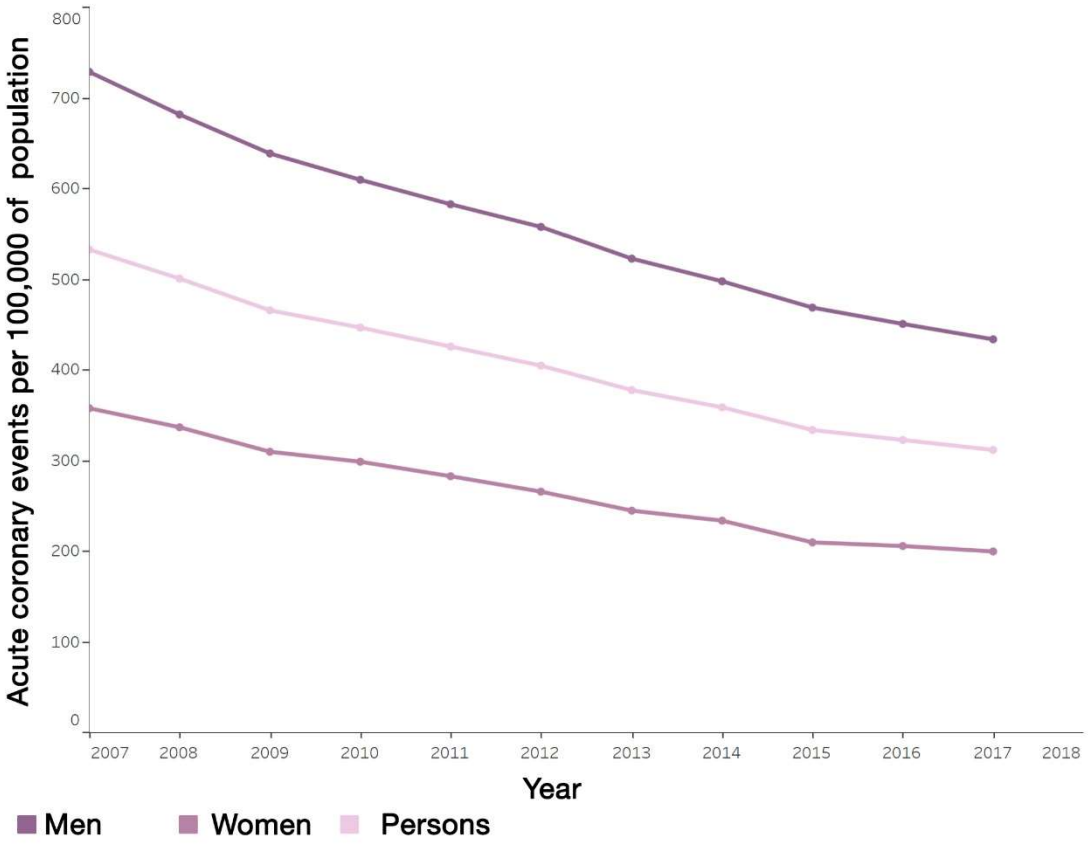

Figure 2. Acute coronary event trends in 2007 - 2017 of Australians over the age of 25 (Australian Institute of Health and Welfare, 2020)

Approximately 126 million individuals were affected by coronary heart disease, estimating 1,655 per 100,000 persons in 2017. Therefore, circa of 1.72% of the world's population was estimated with CHD (Khan, et al., 2020). Statistical analysis presented that around nine million deaths were attributed to CHD, projected as the leading cause of mortality worldwide (Khan, et al., 2020). High income countries such as Germany, United Kingdom, Denmark and Finland moved down in ranks of CHD prevalence, whilst Eastern European countries such as Latvia, Czech Republic, Bulgaria and Lithuania moved up in ranks (Khan, et al., 2020).

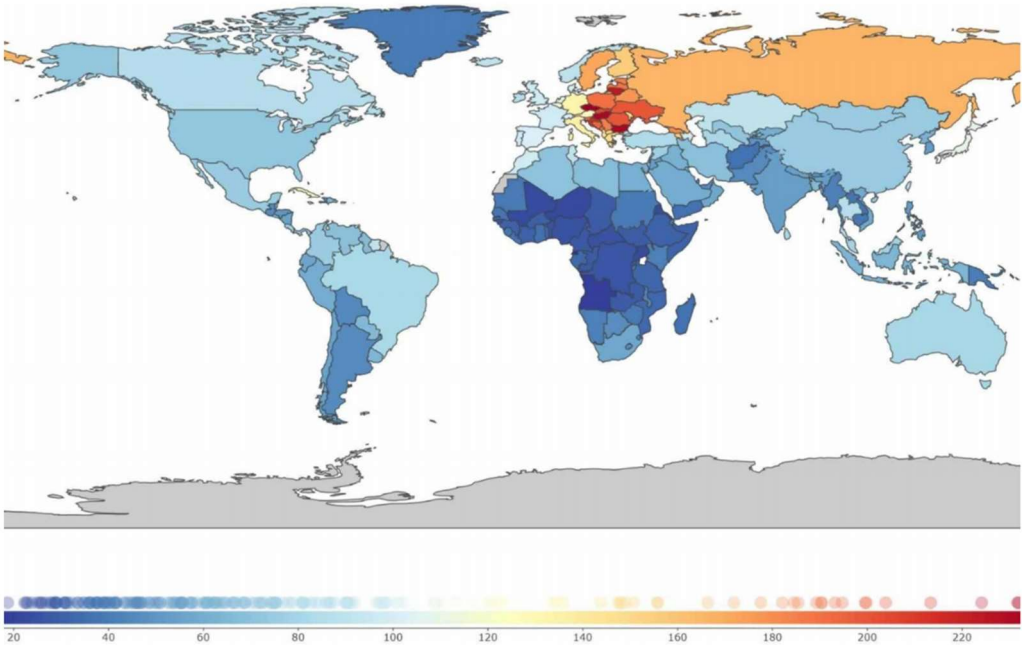

Figure 3. Global distribution of coronary heart disease per 100,000 (Khan et al., 2017)

The male sex is a risk factor in CHD prevalence compared to women and this difference is present in all age groups. Age onset of CHD prevalence is also shown earlier in men, and age distributions indicated that with the increase in age, incidences and prevalence of CHD also increased (Khan, et al., 2020).

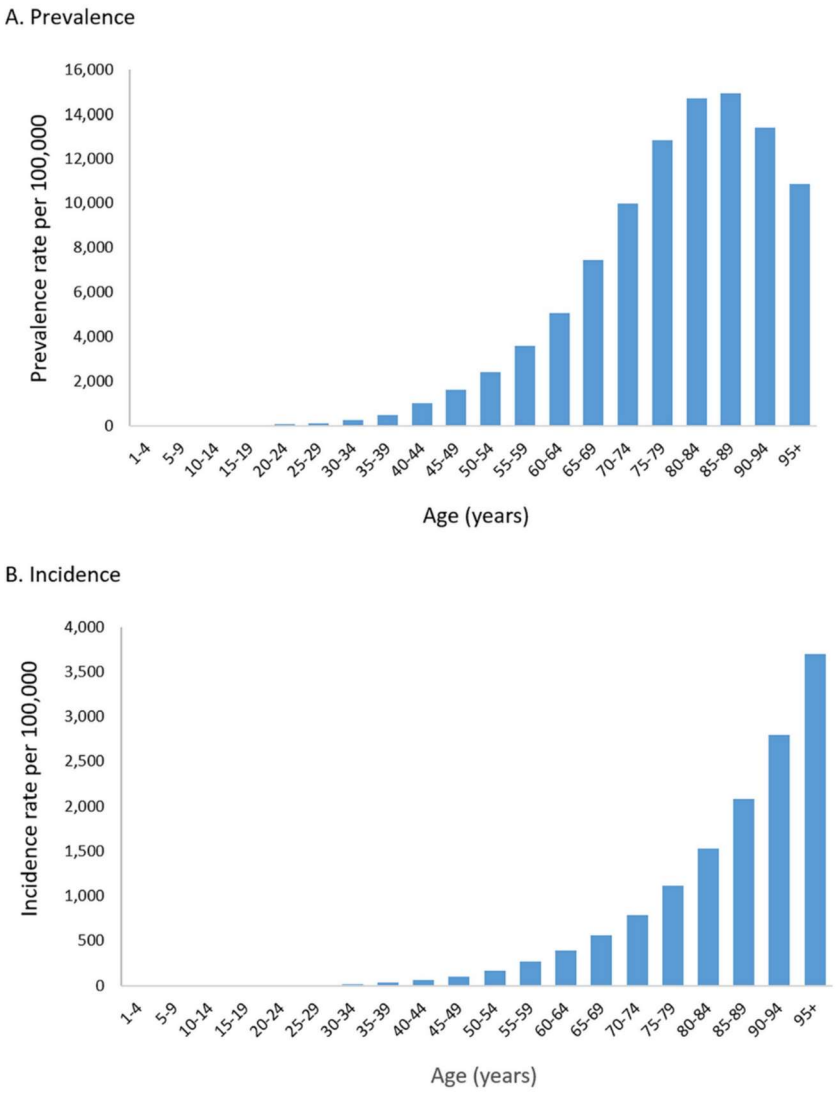

Figure 4. Worldwide (A) Prevalence and (B) Incidence in CHD age distribution (Khan et al., 2017)

6.2 Pharmacology

The chemical structures of various statins are shown in Figure 5. Its' structure can be generally categorised into three parts: the substrate analogue, a hydrophobic ring structure and side groups on the rings. The portion of the molecule that involves this substrate analogue can be in closed ring lactone form (e.g lovastatin) or open-chain form (e.g pravastatin) which targets the enzyme substrate, HMG-CoA (Gaw, et al., 1999). The complex hydrophobic ring structure is of use to allow tight binding onto the reductase enzyme. The side groups classify the solubility properties of the statin, thus its pharmacokinetic properties. The hydrophilic properties are a result of the polar hydroxyl group present in pravastatin and the methane sulphonamide group in rosuvastatin (McTavish & Sorkin, 1991). This polar methane sulphonamide group gives the molecule a comparably low lipophilicity. The additional hydrogen bond in rosuvastatin between the sulfone oxygen atom and the Ser^{565} enzyme as well as the unique polar interaction between

the enzyme Arg^{568} side chain and the electronegative sulfone group allows this statin to have the greatest binding interactions with HMG-CoA reductase. This trait can be similarly attributed to atorvastatin, involving its carbonyl oxygen atom. It can be inferred that greater bonding properties constitutes an increased potency of the statin to the enzyme. Both in vitro and in vivo studies of animal models, suggest that rosuvastatin inhibits hepatic cholesterol synthesis more effectively than other statin available in the market (Olsson, et al., 2002).

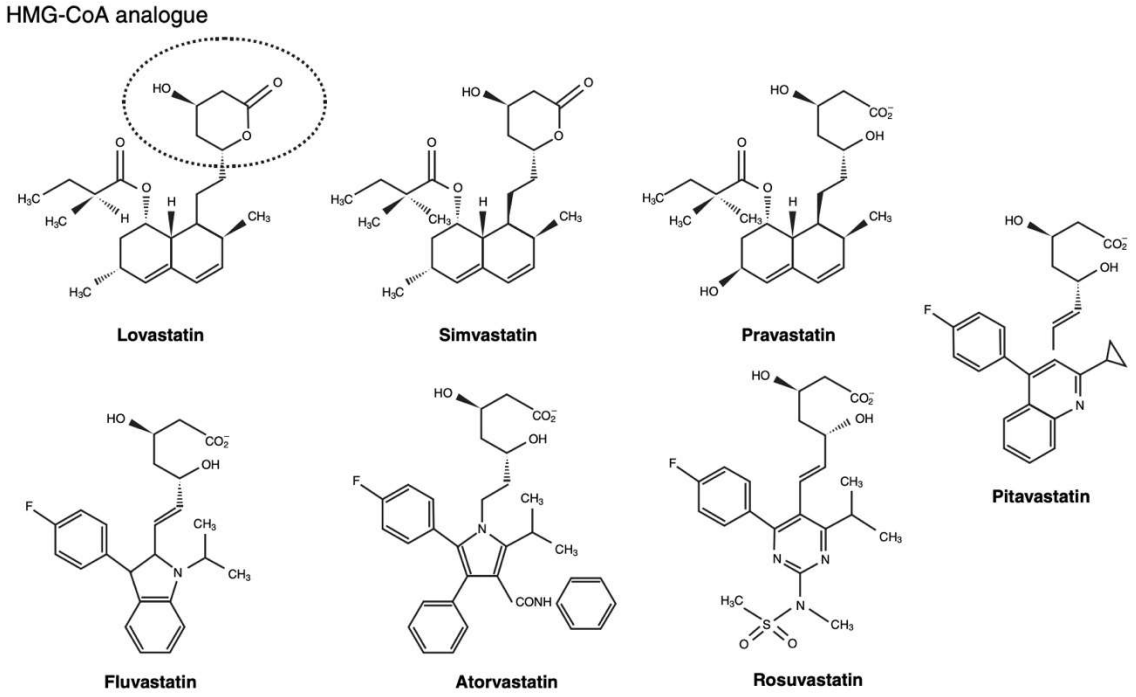

Figure 5. Chemical structures of statins (PubChem, 2020)

The rosuvastatin (rosuvastatin calcium) drug is administered as a calcium salt in patients. The chemical name of rosuvastatin is bis[(E)-7-[4(4-fluorophenyl)-6-isopropyl-2-[methyl(methylsulfonyl)amino] pyrimidin-5-yl](3R,5S)-3,5-dihydroxyhept-6-enoic acid] calcium salt (PubChem, 2020). The empirical formula for rosuvastatin calcium is $(C_{22}H_{27}FN_3O_6S)_2Ca$ with a molecular weight of 1001.14 g/mol (U.S. Food and Drug Administration, 2005).

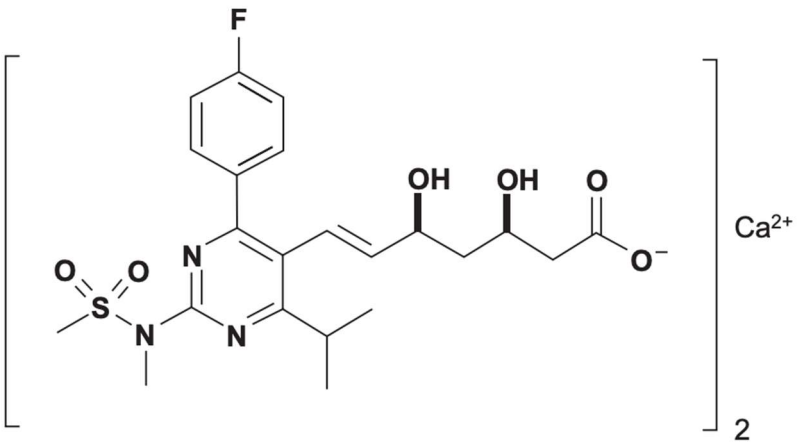

Figure 6. Chemical structure of rosuvastatin calcium (PubChem, 2020)

Rosuvastatin calcium is a white/off-white amorphous powder that is soluble in acetone, acetonitrile, dimethyl formamide, dimethyl sulphoxide; slightly soluble in ethanol and sparingly soluble in water and methanol. Rosuvastatin calcium can be administered in patients as tablets containing 5, 10, 20 and 40mg of rosuvastatin. Additionally, inactive ingredients present in the tablet are presented in Table 1 (RXList, 2017).

Table 1. Inactive ingredients present in Rosuvastatin calcium (RXList, 2017)

Inactive ingredients		
FD&C Blue No. 2	dibasic calcium phosphate dihydrate	magnesium stearate
FD&C Yellow No. 5	crospovidone,	microcrystalline cellulose
FD&C Yellow No. 6	hypromellose	titanium dioxide
FD&C Red No. 40	lactose monohydrate	triacetin

6.3 Pharmacodynamics

6.3.1 LDL-C inhibition and enhancement of its receptor expression

Rosuvastatin, as aforementioned, is a selective and reversible competitive inhibitor of the enzyme HMG-CoA reductase, a widely established mechanism of action of statins. HMG-CoA is converted to mevalonic acid early in the pathway of cholesterol biosynthesis when the HMG-CoA reductase binds to its active site. X-ray crystallography analyses indicates that the rosuvastatin moiety competitively binds onto the HMG-CoA reductase enzyme, via polar and ionic interactions, sterically preventing the native substrate from binding onto the active site (Olsson, et al., 2002). It consequently assists in reducing the production of mevalonate. The decrease in hepatic sterol (cholesterol) synthesis thereby leads to the decrease in total concentration of hepatocellular cholesterol. As biosynthesis of cholesterol is chiefly regulated by hepatocellular cholesterol concentration, the hepatocytes (residing in the liver) will respond to the decreased intracellular cholesterol by increasing the synthesis of the LDL-receptors on its cell surface, enhancing the synthesis of hepatic LDL reuptake. This results in an increased extraction or fractional catabolism of the LDL and decreased LDL-C concentration and total cholesterol (Maron, et al., 2000). Additionally, statins are beneficial with lipid parameters such as increasing hepatic output of high-density lipoprotein cholesterol (HDL-C) and decreasing triglycerides and very low-density lipoprotein cholesterol (VLDL-C) (Maron, et al., 2000).

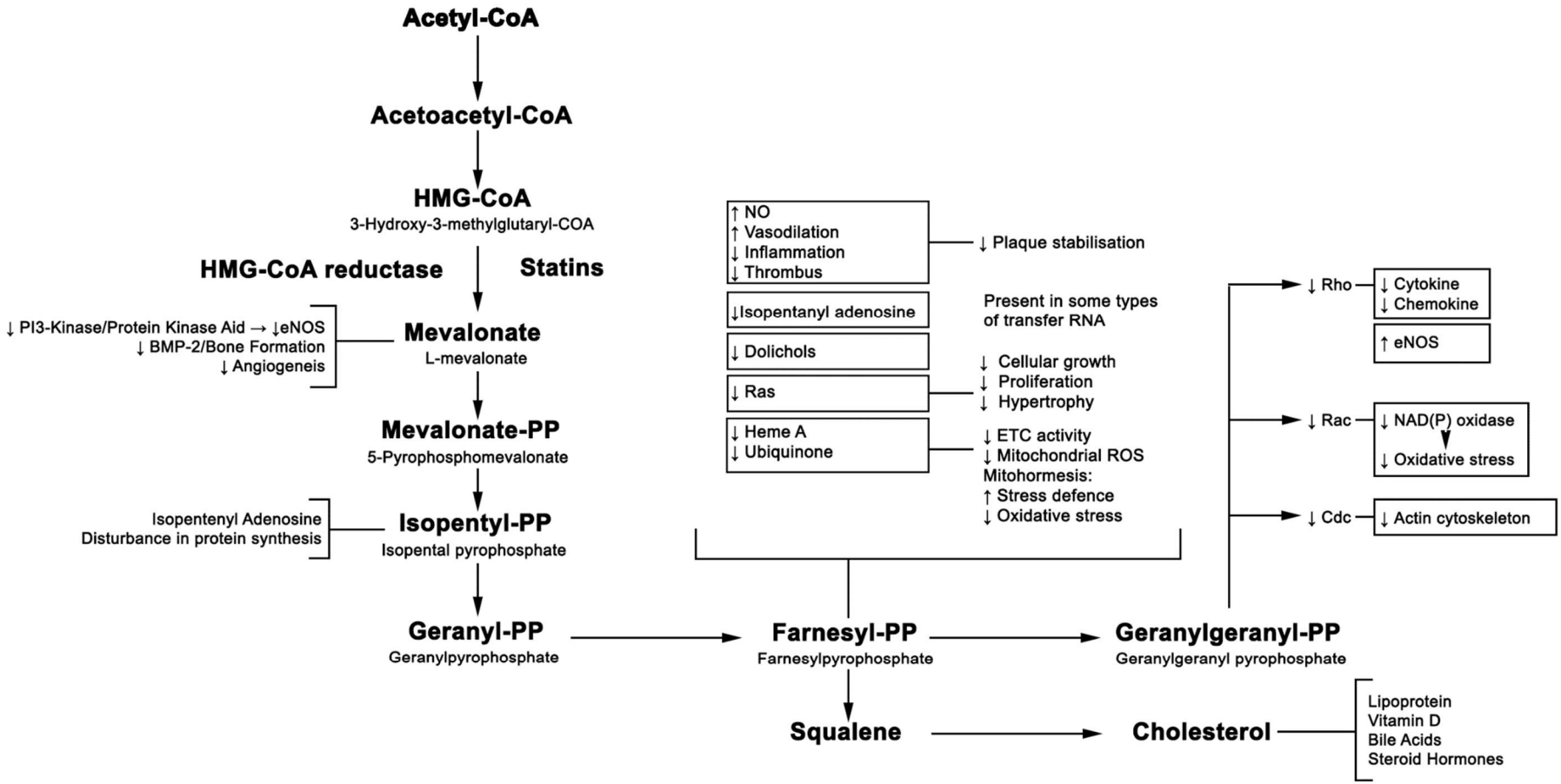

Figure 7. Regulation of the Rho GTPase cycle through statin therapy

By inhibiting HMG-CoA reductase, statins potentially inhibit the synthesis of isoprenoid intermediates, like geranylgeranyl pyrophosphate (GGPP) and farnesyl pyrophosphate (FPP). Several studies have revealed a decrease in prenylated and membrane-associated forms of Ras, Rho, Rac, Rap and nuclear lamins with statin treatment. Prenylation is described as a lipid modification where the geranylgeranyl (20-carbon) and farnesyl (15-carbon) moiety is transferred to the target protein, called geranylgeranylation and farnesylation, respectively. This essential post-translational modification is involved in various cellular processes including intracellular protein trafficking, cell metabolism, cell proliferation and differentiation. Long-term usage of statins disrupts the balance of protein geranylgeranylation and farnesylation by isoprenoid depletion and have exhibited adverse effects such as myopathy and liver injury (Chalasani, 2005) (Zhao, et al., 2020).

6.3.2 Statin pleiotropy

Statin therapy suggests that rosuvastatin, like other statins, have pleiotropic effects of statins extend beyond its effects on serum cholesterol levels. Pleotropic effects may be unrelated to the primary mechanism of action and are usually not anticipated. Therefore, these effects may be beneficial, neutral or undesirable for the human body. There are observed improvements in nitric oxide bioavailability, endothelial function, anti-thrombotic, anti-inflammatory and antioxidant effects with the use of statins. Some of these observed outcomes through clinical studies may be due to direct cholesterol lowering

Disease / Impairment	**Pleiotropic effects of statins (rosuvastatin)**
Dementia	• Changes in cellular cholesterol distribution that are induced in the brain (Liao & Laufs, 2005)
Cardiac contractile dysfunction	• Reduction in arterial pressure • Improvement in systemic & regional haemodynamics (Ikeda, et al., 2003)
DNA damage	• Antioxidative effects by inducing expression of antioxidant defence enzymes (Neto-Ferreira, et al., 2011)
Gastrointenstinal	• Decrease in cholecystectomy for gallstones (Giroux, et al., 1993) • Decrease in pancreatitis with normal triglycerides (Sánchez-Quesada, et al., 1999)
Kidney disease	• Decrease in creatinine with normal and abnormal renal function (Heart Protection Study Collaborative Group., 2002) (Witztum & Steinberg, 2001) (Giroux, et al., 1993)

Ischemia/Reperfusion Injury	• Reducing injury by preventing cardiomyocyte and coronary endothelial cell damage (Di Napoli, et al., 2005)
Pneumonia	• Decrease in incidence
Venous thromboembolism	• Decrease in incidence
Multiple sclerosis	• Decrease in whole brain atrophy
Rheumatoid arthritis	• Improved disease activity score • Decrease in inflammatory markers
Periodontal disease	• Decrease in periodontal inflammation (Subramanian, et al., 2013)

Gnotobiotic models, which are defined as animals that are cultured in defined microbial lineages or axenic conditions, are a common and efficient tool used in discovering molecular interactions between the host and the gut microbiome. It is a system which accounts for all aspects required to make powerful inferences with human health. The effects of statin pleiotropy cannot be easily or conclusively deduced as it is difficult to emulate a gut model in this manner. This can also be inferred to the implications of statins on gut health. If possible, producing a model that is a gnotobiotic system can directly account for the causes and effects of statins on microbiota and their implications on gut health.

An increasingly productive option is to thus study the complex biological processes that occur using mathematical and computational modelling. This computational model can serve to design a reactor, as researched in Semester 1, 2020, where seeding microbiota samples from gut can assist in producing a physical bioreactor that can emulate and grow a microbiota biome. It is advantageous as this process can be experimented without a further requirement of human trials.

6.4 Statin Therapy

6.4.1 Atherosclerotic vascular disorders

Atherosclerosis is a disease where arteries acquire plaque build-up, such as fats and cholesterol. The hardening of plaque leads to narrow arteries, thus limiting oxygen-rich blood flow. Through the combined reduction of lipids, matrix metallopeptidase (MMPs) and macrophages, statins reduce the prevalence of inflammatory cells in atherosclerotic plaques. Zhou et al., reported that statins are able to lower the growth and proliferation of macrophages, interactions between monocytes and the vascular wall and monocyte chemotaxis (Zhou & Liao, 2009). Statins further reduce mRNA in cyclooxygenase (COX), a mechanism that is common in anti-inflammatory drugs (Zhou & Liao, 2009). Statins reduce the production of inflammatory markers such as chemotactic cytokines, interleukin-1β and tumor necrosis factor-α. Furthermore, it is reported that statins disturb the oxidative stress/inflammatory cycles due to the release of inflammatory mediators and decrease of

lipid peroxidation (Inoue, et al., 2000).

As aforementioned, statins inhibit the isoprenylation of Rac and Rho, which in turn improved endothelial function. Additionally, the ROCK pathway is inactivated leading to an increased eNOS activity. 'Endothelial nitric oxide synthase' or eNOS, is an isoform that is responsible for the production of vascular nitric oxide (Martínez-González, et al., 2001). As statins directly increase eNOS activity, bioavailability of nitric oxide (NO) also increases. NO is a signalling molecule that maintains metabolic and cardiovascular homeostasis, whereby the bioavailability indicates positive utilisation and production of endothelial NO in organisms. The decrease in NO will introduce lipid infiltration, oxidative stress, alteration of the vascular tone and inflammatory factors which plays a major role in endothelial dysfunction (Chen, et al., 2018). The inactivation of the ROCK pathway activates the protein kinase Akt, that has been correlated with accelerating the angiogenesis process (Inoue, et al., 2000). Administering rosuvastatin exhibited increased levels of bone marrow-derived stem cells circulation in humans (Kamio, et al., 2010). This mechanism may contribute to improving cardiac regeneration and repair (Mathur, et al., 2008). Statins are reportedly beneficial to hypertensive patients with a history of myocardial infarction and cerebral ischemia due to its regulation of the sympathetic and vagal outflow in the central nervous system (Bellosta, et al., 2004). Statins have shown to induce mitohormesis due to the cardioprotective mechanisms of statins. Such responses have been shown to enhance the lifespan in different animal models by improving the immune system and metabolic activities (Bárcena, et al., 2018).

6.4.2 Stroke

Although controversial and not wholly established in studies, statins have been shown to reduce the risk of stroke. In ischemic strokes, elevated LDL-C and cholesterol are identified as risk factors discussed across many epidemiological studies. In the JUPITER trial, which prompted statin therapy with rosuvastatin use, the reduction in risk was observed as 48% (Everett, et al., 2010). Similarly, studies by the Heart Protection Study and others states that statins reduce the risk of stroke by 25% (Collins, 2003). Another trial has supported that statin therapy with other non-statin cholesterol medication, such as simvastatin and ezetimibe have exhibited a reduction in risk of ischemic stroke by 21% (Baigent, et al., 2009).

6.4.3 Other disorders

Bifulco et al., stated the potential of statins as treatment for neurological disorders such as Parkinson's disease, primary brain tumours, multiple sclerosis and Alzheimer's disease. Anti-inflammatory, antioxidant, anti-platelet activities and the increase of NO bioavailability have shown to contributed to the listed disorders. Statins have presented beneficial effects in rheumatoid arthritis, attributed to the downregulation of chemokines

and cytokines (Agarwal, et al., 2010).

Healthy patients intaking rosuvastatin had a decreased the risk of symptomatic venous thromboembolism VTE by nearly 50% (Glynn, et al., 2009). Statin administration have been beneficial in seasonal and avian H5N1 influenza, owing to its anti-inflammatory, cardioprotective and immunomodulatory effects (Fedson, 2006).

Statins intake have been stated to indirectly or directly block the oxidative stress increase in insulin resistance, steroidogenesis and interstitial cell proliferation, which has benefited women with polycystic ovary syndrome (PCOS). Oxidative stresses are recognized to play a major role in the pathophysiology of PCOS and other disorders (Kodaman & Duleba, 2008) (Rzepczynska, et al., 2009).

6.5 Pharmacokinetics

The mechanism of action across all statins is the same, however their lipid-modifying efficacy, chemical structure and pharmacokinetic profiles differ. The variance in chemical structures influences the water solubility, thus adsorption, metabolism, excretion and distribution. Statins that have been derived from fungal metabolites such as pravastatin, lovastatin and simvastatin have an elimination half-life of 1-3 hours. Conversely, fully synthetic compounds such as rosuvastatin, atorvastatin, pitavastatin and fluvastatin have a wider range of elimination half-life, spanning from 1 hour (fluvastatin) to 19 hours (rosuvastatin). Relatively lipophilic statins such as atorvastatin, lovastatin, pitavastatin, fluvastatin and simvastatin are more susceptible to be metabolised by the cytochrome P450 system. On the contrary, hydrophilic statins such as rosuvastatin and pravastatin undergo minimal hepatic metabolism. Cytochrome P450 (CYP) is a haemoprotein, is a protein containing a haem prosthetic group, which plays a major role in the metabolism of drugs and is biosynthesised in the liver and bone marrow.

Table 2. Pharmokinetic properties of statins (Gaw, et al., 1999)

	CYP450 metabolism and isoenzyme	**Solubility**	**Protein binding (%)**	**Active metabolites**	**Elimination half-life (hour)**
Atorvastatin	Yes, 3A4	Lipophilic	98	Yes	14
Fluvastatin	Yes, 2C9	Lipophilic	>98	No	1.2
Lovastatin	Yes, 3A4	Lipophilic	>95	Yes	3
Pravastatin	No	Hydrophilic	~50	No	1.8
Rosuvastatin	Yes, 2C9	Hydrophilic	90	Few	19
Simvastatin	Yes, 3A4	Lipophilic	95-98	Yes	2

	Bioavailability (%)	Dosing time	Effect of food (Bioavailability)	Renal excretion (%)
Atorvastatin	12	Any	Decrease	<5
Fluvastatin	24	Night	Decrease	6
Lovastatin	5	With meals (morning & evening)	Increase	10
Pravastatin	18	Night	Decrease	20
Rosuvastatin	20	Any	No effect	10
Simvastatin	5	Evening	No effect	13

All statins are selective to take effect in the liver, which is an organ that detoxifies and facilitates the excretion of xenobiotics (foreign drugs or chemicals) by the enzymatic conversion of lipid-soluble compounds to a more water-soluble compound (McDonnell & Dang, 2013). This is principally due to the effectiveness of the first-pass effect, a phenomenon where the substance reaches the liver before other organs as it enters the hepatic portal system through the portal vein (Rowland & Malcolm, 1972). Additionally, the hepatic (liver-related) uptake in lipophilic statins can be attributed to its passive diffusion through the cell membranes of hepatocytes, which are the key epithelial cells in the liver. Alternatively, the hepatic uptake of hydrophilic statins is due to an active carrier-mediated process. Hydrophilic statins such as rosuvastatin and pravastatin have additionally shown to have a greater binding selectivity in liver cells, or hepato-selectivity, compared to their lipophilic counterparts, thus a reduced probability of uptake from peripheral cells. Rosuvastatin has the greatest efficacy of LDL cholesterol reduction, according to clinical studies, followed by atorvastatin, simvastatin and pravastatin (Schachter, 2005).

When the rosuvastatin drug is administered in patients, clinical pharmacology studies suggest that the peak plasma concentrations (C_{max}) were reached 3-5 hours after oral dosage. The C_{max} and area under the plasma concentration-time curve (AUC) additionally increase proportionally with dosage amount.

6.5.1 Special Population

A population pharmacokinetic analysis disclosed that there are no clinically relevant differences observed in race (Caucasian, Black, Hispanic or Afro-Caribbean groups). The Food and Drug Administration has recommended that Asian patients should intake a dosage reduction of 5mg due to an approximate two-fold elevation in Asian subjects compared with Caucasian control group in a pharmacokinetic study conducted (U.S. Food and Drug Administration, 2005). Recent studies suggest that there is no significant difference in healthy Asian and Caucasian subjects. Instead Wu, et.al, proclaims that for precision medicine dosing, the genetic variations (SLCO1B1 and ABCG2 polymorphisms) are better predictors of rosuvastatin exposure, than just ethnicity alone (Wu, et al., 2017). Other special population studies such as gender, geriatric and paediatric (heterozygous FH presence) and the time of dosage (morning or evening) also showed no clinically relevant

differences. In patients with mild to moderate impairment in renal insufficiency, the plasma concentrations of rosuvastatin was not influenced with a dosage of 20mg rosuvastatin administered for 14 days. Between healthy subjects and patients with severe renal impairment, the plasma concentration of rosuvastatin were clinically significant where there was a substantial increase by around three-fold (Fellström, et al., 2007). According to clinical studies available, Table 3 identifies the changes in patients that have impairments and diseases that consume rosuvastatin daily.

Table 3. Changes in patients with renal insufficiency, haemodialysis & hepatic insufficiency taking rosuvastatin

Impairments/Disease	**Steady state plasma concentrations (mL/ min/1.73m^2)**	**Peak plasma concentration (C_{max})**	**Area under plasma concentration-time curve (AUC)**
Severe renal impairment	Creatinine clearance increase Healthy: 30 Impairment: >80	-	-
Chronic haemodialysis	60	-	-
Chronic alcohol liver disease	40	-	-
Child-Pugh A disease (chronic liver disease)	-	60% increase	5% increase
Child-Pugh B disease (chronic liver disease)	-	100% increase	21% increase

The peak plasma or drug concentration (C_{max}) is an indication of assessment into the rate of adsorption. Conversely, area under the plasma concentration-time curve (AUC) in steady state studies is an indicator for the extent of adsorption (U.S. Department of Health and Human Services, 2013). These are pharmacokinetic measures regarding the rate and extent of exposure for patients that uptake the rosuvastatin drug with additional impairments or disease. This can convey the efficacy of the drug under certain conditions. The bioequivalence of adsorption rates can be further obtained with the use of the C_{max}/AUC ratio, which is recommended by Endrenyi as a clearer measure of adsorption rate (Endrenyi, et al., 1991). It was concluded by the Food and Drug Administration that administering rosuvastatin with food showed a decrease of drug adsorption (C_{max}) by 20% in pharmacokinetic studies, but no evident effect on the extent of adsorption (AUC) (U.S. Department of Health and Human Services, 2013). Regardless of the time, it was assessed that there was a significant reduction in LDL-C and no change in plasma concentrations with rosuvastatin uptake in healthy patients (McTaggart, et al., 2001) (U.S. Food and Drug Administration, 2005)

6.6 Influence of the gut microbiome on the efficacy of statins

In comparing and assessing studies that are available, those that were taken into consideration have addressed the influence of the gut microbiome with the therapeutic effects of statin intake and evaluated the enteric bacterial composition of sample patients. The two outcomes that have been evaluated are:

a) The role of statins in the gut microbial environment modulation
b) The potential influence that the gut microbial composition has on the lipid-lowering efficacy of statins

6.6.1 Human studies

A study conducted by Liu et al., examined the efficacy and lipid-lowering effects of rosuvastatin in association with the diversity and species abundance present in the gut microbiome. A total of 64 men and women with primary hypercholesterolaemia orally consumed 10mg of rosuvastatin for up to 8 weeks. Conversely, Sun et al., conducted a comparatively similar study design in China with stark differences – atorvastatin was the statin agent used with an increased drug dosage of 20mg, a longer duration of treatment (12 weeks) and a greater sample of subjects were employed. It can be noted that these study designs were quasi-experimental which compared treated subjects as responders and poor responders. Summary of the studies have been included in Table 4.

Table 4. Human studies examining the efficacy of statins in the gut microbiome

Study details	Sample & Treatment	Study design	Sequencing method
• Liu et al., 2018 (Liu, et al., 2018) • China	• Men (45) • Women (19) • Primary hypercholesterolaemia • Rosuvastatin, 10mg (oral) • Duration: 4-8 weeks	• Measurement: Blood LDLc, HDLc, Triglyceride and Total cholesterol at week 0, 4 & 8 • Faecal collection: week 0 • After treatment: Sample groups divided based on blood lipid levels. Group 1: BLL dropped to normal levels (Week 4) Group 2: BLL maintained above normal levels	• Amplification by PCR • V3 – V4 regions of 16S rRNA gene
• Sun et al., 2018 (Sun, et al., 2018) • China	• Men (202) • Newly diagnosed hypercholesterolaemia • Atorvastatin, 20mg (oral) • Duration: 12 weeks	• Measurement: Blood LDLc, at week 0, 4, 8 & 12. • Faecal collection: week 0 • After treatment: Sample groups divided based on LDLc levels. Group Statin Sensible: < 100mg/dL Group Statin Resistant: ≥ 100mg/dL	• Amplification by PCR • V3 – V4 regions of 16S rRNA gene
• Khan et al., 2018 (Khan, et al., 2018) • Saudi Arabia	• Men & women (42) • Hypercholesterolaemia • Atorvastatin, 20mg (oral) • Duration: N/A	• Enrolled subjects divided into 3 groups HP: Statin-naïve (15 subjects) At-HP: Atorvastatin treatment for past 2 years (27 subjects) HS: Control group (19 subjects)	• Amplification by PCR • V3 – V4 regions of 16S rRNA gene

		Results	
Study details	Bacterial taxonomy	Bacterial diversity	Conclusion by author
• Liu et al., 2018 • China	• Phylum Group 1: Higher amount of Firmicutes Group 2: Increased amount of Actinobacteria • Family Group 1: High amount of Bifidobacteriaceae, Lactobacillaceae & Ruminococcaceae Group 2: Increased amount of Bacteroidaceae, Enterobacteriaceae, Streptococcaceae, Pseudomonaceae and other bacteria that produce endotoxins	• Group 1 had greater bacterial diversity compared to Group 2. • Both groups had very different compositions of the gut microbiome	• Gender could influence microbial diversity • Gut microbiota can influence statin treatment in patients with dyslipidaemia • Modulation of microflora in the gut will assist in statin effectiveness • Higher gut biodiversity microbiota was associated with the rosuvastatin hypolipidemic effect
• Sun et al., 2018 • China	• Phylum Group SS: Higher amount of Firmicutes • Genus Group SS: Higher amount of Bifidobacterium, Eubacterium, Faecalibacterium & Lactobacillus Group SR: Higher amount of Clostridium	• Group SS presented a greater bacterial diversity compared to Group SR.	• Higher gut biodiversity associated with the statin sensitive response • Gut microbiota can be used to predict statin response of patient • Transplanting specific gut microbes can achieve greater therapy efficacy • Diet supplemented with probiotics may improve statin treatment efficacy in hyperlipidaemic patients
• Khan et al., 2018 • Saudi Arabia	• Phylum HP: Higher amount of Proteobacteria At-HP: Increased amount of Firmicutes • Family HP: Increased amount of Prevotellaceae and Enterobacteriaceae At-HP: Higher amount of Verrucomicrobiaceae and Ruminococcaceae	• HS present greatest bacterial diversity, followed by HP and then At-HP being the least diverse • HS and At-HP exhibited similar taxonomical properties	• With treatment, HP and At-HP had shifted its bacterial composition towards an anti-inflammatory gut microbial environment, despite exhibiting less bacterial diversity

In the human studies performed, all three studies had failed in reporting a cohesive methodology in the recruitment of sample patients, leading to a selection bias. Liu et al., was able to minimise the selection bias by consecutively enrolling subjects, allowing the potential patients have equal chances of being sampled. It can be inferred that Liu et al's., sampling was a better representative of the target population. In Khan et al's. study, filling a questionnaire will allow for a memory bias.

From the studies conducted by Liu et al., and Sun et al., it can be extracted that patients presenting higher levels of bacteria belonging to the Firmicutes phylum and increased amounts of known gut commensals, such as *Bifidobacterium* and *Lactobacillus*, had a better statin response (LDLc decrease of 58.5%). Bacteria in relation to Firmicutes phylum are

able to contribute to the metabolic process of compounds that display anti-obesity and anti-diabetic properties (Eid, et al., 2017). It is yet unclear how the gut microbe environment is benefitted by statin treatment. Dias et al., comments that this may be due to a broader interaction of the gut microbiome in association with the host cell properties to alter drug receptor modulators and enzymes that are responsible in metabolising statins. Studies conducted by Sun et al., and Liu et al., did not provide information regarding supplementary medication that may influence the gut microbiome composition, smoking or exercise habits and probiotics consumption.

Patients which exhibited a positive response to statin therapy in Sun et al's., studies also showed increased levels in Faecalibacterium and Eubacterium, bacterial genera that are well-documented to decrease cholesterol levels in hosts. During the fermentation of complex carbohydrates, microbial-derived metabolites like short chain fatty acids (SCFA) are produced. This affects various host processes such as colonic pH, energy utilisation and host-microbe signalling, consequently affecting gut motility and microbiota composition (Musso, et al., 2011). SCFAs are integral in maintaining the integrity of the intestinal barrier and can lower serum lipid levels by liver redirection or blocking cholesterol synthesis. Bacteria such as *Faecal prausnitzii* and *Eubacterium rectale* are positively correlated with SCFAs [54]. Additionally, a greater gut microbial diversity had been related with an improved response to statin treatment. It can be deduced that gut microbial flora plays a potential role in statin action.

Khan et al., investigated the potential influence of statins on the composition of the gut microbiome. Hypercholesterolaemic patients that were treated with atorvastatin were observed to develop an anti-inflammatory profile, where the bacterial proportions of *Faecalibacterium prausnitzii* and *Akkermansia muciniphila* had been increased. F prausnitzii have been noted to decrease pro-inflammatory cytokines such as TNF-α and IL12 and increase the IL10 anti-inflammatory cytokine. However, an animal study by Schneeberger et al., established *A. muciniphila* was not correlated with inflammatory markers, adiposity and lipid synthesis. Conversely, untreated hypercholesterolaemic patients showed a relative abundance in Enterobacteriaceae, *Desulfovibrio* spp. and Proteobacteria, which are regarded as pro-inflammatory bacteria. The statin treated group had restored a healthier profile that was comparable with the control group (healthy subjects), revealing that statin therapy can be a driving force to gut microbiome modulation. Any cause-effect relationships cannot be made in this cross-sectional study due to the following reasons:

1) Bacterial composition before treatment is unknown
2) Reliance on patient's questionnaires are a confounding factor
3) Opposite trends, like *A. muciniphila* have no correlation to inflammatory markers

6.6.2 Animal studies

There is limited evidence concerning the bi-directional effects of the microbiota and statins, particularly rosuvastatin, therefore murine models were deliberated but may hamper direct

comparisons. Mouse/rat models are unable to wholly reproduce human systems or reflect the interplay between host and gut microbiome, as it is host specific. A realistic gut microenvironment is difficult for mouse models to emulate as multiple human background factors such as medical history and diet contribute to shape individual-specific gut microbiomes. However, murine models allow for the evaluation of specific interactions established by the gut microbiota, providing an understanding drug metabolism pathways and pathological mechanisms. A summary of animal studies with rosuvastatin therapy is listed in Table 5.

Table 5. Animal studies examining the efficacy of rosuvastatin in the gut microbiome

Study details	Sample & Treatment	Study design	Sequencing method
• Wang et al., 2018 (Wang, et al., 2018) • China	• Male SPF SD rats • Rosuvastatin, 10mg kg^{-1} body weight (oral) • Duration: 4 weeks	• Measurement: Blood LDLc, HDLc, Triglyceride and Total cholesterol at week 0, 4 & 8 • Faecal collection: week 0, 2 & 4 weeks • Subjects divided into 3 groups in dysbiotic rat model Group 1: Rosuvastatin & antibiotic Group 2: Rosuvastatin Group 3: Saline	• Amplification by PCR • V3 – V4 regions of 16S rRNA gene
• Nolan et al., 2017 (Nolan, et al., 2017) • China	• Female C57BL/6J mice • Rosuvastatin, 9.3mg kg^{-1} body weight (oral) • Duration: 4 weeks	• Measurement: Blood LDLc, • Subjects were fed a high fat diet for 2 weeks prior to rosuvastatin intake Group 1: sterile water with rosuvastatin Group 2: sterile water	• Amplification by PCR • V4 – V5 regions of 16S rRNA gene

	Results		
Study details	**Bacterial taxonomy**	**Bacterial diversity**	**Conclusion by author**
• Wang et al., 2018 • China	• Group intaking rosuvastatin and antibiotic had diminished levels of genus *Bifidobacterium* and *Lactobacillus* compared to exclusively rosuvastatin group	• Group 1 had a reduced bacterial diversity compared to Group 2 & 3 initially • There was no difference in gut microbial diversity between all 3 groups at week 4 • At week 4, gut microbial composition of Group 1 were different compared to Group 2 & 3, which were similar to one another	• Rosuvastatin's lipid-lowering ability can be influenced by intestinal microflora that has been disrupted
• Nolan et al., 2017 • China	• *Bacteroidetes* and *Firmicutes* were dominant in both groups	• Group 1 exhibited significantly lower microbial diversity compared to Group 2 • Faecal analysis: no significant differences • Distinct cluttering of gut microbiota in caecal	• Rosuvastatin altered the gut microbiota • Alterations may also be due to host responses, conclusion is ambivalent

samples, compared to faecal samples

A study by He et al., where simvastatin was administered in male mice, evaluated the statin responses of a dysbiotic mouse model compared to a nonsymbiotic model (He, et al., 2017). It was observed that the hypolipidemic effect of simvastatin exerted numerous beneficial actions such as stimulating specific hepatic proteins that regulate bile acid synthesis, decreasing phospholipid levels and doubling lithocholic acid concentration. Lithocholic acid is a bile acid that solubilises fats for adsorption. The alteration of the hypolipidemic effect of simvastatin may be due to:

a) The proteins liable for bile acid synthesis are impaired in gut microbial dysbiotic environment (simvastatin stimulates the expression of these proteins)
b) The composition of anaerobic bacteria was altered in the presence of antibiotics (anaerobic bacteria metabolises simvastatin)
c) Lithocholic acid that have been derived by Clostridium may have increased concentrations in simvastatin-treated groups compared with antibiotic treated groups

Simultaneous administration of antibiotics and simvastatin resulted in impairment of these actions, denoting that gut microbial composition is influential in statin activity. However, there is a lack of research that relates bile acid homeostatic protein processes to the hypolipidemic effects of statins, and how these interactions are influenced by the gut microbiome.

Similarly, Wang et al's., studies revealed that after 4 weeks, the group that was treated with antibiotics and statins and statin monotherapy, displayed cholesterol levels that were much lower than the water group. This is palpably contrasted in the initial two weeks, where the AB + Statin group presented elevated levels of cholesterol. This demonstrates that the efficacy of statins are reduced in a decreased microbial biodiversity, but also that with time, the statin hypolipidemic effects re-emerge after microbial community replenishment. These discrepancies were explained by the bacterial composition of *Bifidobacterium* and *Lactobacillus* in the Statin group when compared to the AB + Statin group. These bacteria are potential regulators of TNF-α and IL6 cytokines (Everett, et al., 2010), which are known to regulate the OATP1B1 rosuvastatin transporter (Collins, 2003).

Multiple studies were considered to evaluate the influence of statins on the gut bacterial composition. Khan et al's., comparison of normal chow diet (NCD) and a high fat diet (HFD) under the influence of atorvastatin, suggested that drug-specific effects did not have a distinct and predictable response on the host health, even in definite bacterial populations. Although the hyper-lipidic diet decreased microbial diversity, there was a clear shift towards a comparable NCD environment. In the HFD group intaking atorvastatin, there was a higher relative abundance of Parabacteroides and Bacteroides genera present. The Parabacteroides genus consists of anti-inflammatory bacteria has shown positive increases, even with varied

atorvastatin dosage (Heart Protection Study Collaborative Group., 2002). Bacteroides genus is linked with the metabolism of bile acid. Khan et al., indicates that careful analysis is required to prescribe statins due to these implications on the host's health.

Table 6. Study evaluating the influence of statins on the gut microbial composition (Caparrós-Martín et al., 2017)

Study details	Sample & Treatment	Study design	Sequencing method
• Caparrós-Martín et al., 2017 (Caparrós-Martín, et al., 2017) • Australia	• Male wild type mice (C57BL.6J) • Atorvastatin, 10mg kg^{-1} body weight (oral) or Pravastatin 10mg kg^{-1} body weight (oral) • Duration: 12 weeks	• Measurement: Blood LDLc, • Faecal collection: week 0, 2 & 4 weeks • Subjects divided into two groups (HFD & NCD) and further 3 minor groups Group 1: No intervention Group 2: Atorvastatin Group 3: Pravastatin	• Amplification by PCR • V3 – V4 regions of 16S rRNA gene

	Results		
Study details	Bacterial taxonomy	Bacterial diversity	Conclusion by author
• Caparrós-Martín et al., 2017 • Australia	• Phyla NCD: Bacteriodetes and Firmicutes predominant Group 2 & 3: Increase in Bacteroidetes and reduction in Firmicutes	• NCD within Group 2 & 3 lower diversity compared to NCD within Group 1 • Atorvastatin had least diversity	• Statin's lipid-lowering ability can be influenced by intestinal microflora that has been disrupted

Caparrós-Martín et al's., study engaged in a similar study design and drug therapy, expressing that statin therapy is potentially the driving force of gut microbiome alterations, proceeding throughout distinct metabolic pathways. Caparrós-Martín et al., informed that no alteration in cholesterol levels were discovered after statin treatment. A lower diversity of S24-7, a family of bacteria within the major taxa, Bacteroidales and a reduction in Firmicutes phylum was also reported after statin treatment. The impairment of butyric acid production levels would indicate a dysbiotic gut. A deregulation in the transport or the synthesis of metabolites can be attested to the amplification in the bile acid pool. The nuclear receptor, pregnane X receptor (PXR), that is found in the intestines and liver, could be responsible for these alterations as they take a role in metabolising diverse substances including bile acids and xenobiotics (Lloyd, et al., 2013) (Cannon, et al., 2004). Ko et al's., analysis on statin activity alongside gram-positive and gram-negative agents, conclude that simvastatin appears to have greatest potency in antimicrobial activity, followed by atorvastatin, rosuvastatin and fluvastatin (Schwartz, et al., 2001). Based on in vitro experiments, it has been assumed that statins employ their modulation on gut microbial communities by directly disrupting bacterial membrane architecture, not just HMG-CoA inhibition or bile acid pool alteration.

Due to the scarcity of evidence available about the relationship between the gut microbiome and statins, it is difficult to make finite cause-effect conclusions. Broader generalisations are challenging due to the lack in number of studies. The animal and human studies presented discrepancies such as type and dosage of statin, duration of treatment, sample collection

times, and the number of subjects that had been enrolled. Patient characteristics, lifestyle characteristics, diet, concomitant medications and diseases were confounding variables that had not been identified. In order to understand the bi-directional relationship between statins and the gut microbiome, it is essential to incorporate homogenous study designs and methodologies to allow for correlations to be formed. Defining the dysbiotic environment by outlining the compositions and overall diversity of the microbial communities in human and animal studies will also assist in understanding the relationship between the two. Although it can be inferred that the influence of statins in patients had been compromised in the presence of gut dysbiosis, evidence is lacking to provide personalised therapeutic treatments based on their gut microbiome composition. Further research is required to form significant correlations between statin treatment and the gut microbiome.

6.7 Statin use for cardiovascular prevention

Raised levels of low-density lipoprotein (LDL) and total cholesterol (TC) are risk factors examined for cardiovascular disease due to atherogenesis. Atherogenesis is defined as the plaque formation in the intima layer of arteries. With progressive lipid accumulation and inflammation of such plaque within the arterial walls is an indication of developing atherosclerosis. Coronary atherosclerotic heart disease, commonly referred to as coronary heart disease (CHD) is the greatest contributor to cardiovascular diseases. As statins reduce the plasma LDL cholesterol, it may be used for both primary and secondary prevention of cardiovascular disease (CVD). Primary prevention encompasses treatment of persons who have not been distinguished with cardiovascular disease, however, is at risk of CVD in the future. Conversely, secondary prevention is the treatment of those with established cardiovascular diseases. It has been demonstrated that statins have an effect in the primary and secondary prevention of coronary heart disease through landmark clinical trials. Further, studies have proposed both pleiotropic and LDL-dependent effects can be observed with statin therapy.

The main findings in individual studies that are available are consistent through a meta-analysis in that with the reduction in 1.0 mmol/L in LDL, it results in a 22% decrease in risk of major vascular events (Baigent, et al., 2009). Statin therapy had demonstrated coronary protection in the elderly for the long-term, with a mean follow-up of 8.6 years (Lloyd, et al., 2013). The Scandinavian Survival Study supports that simvastatin therapy reduced the risk of major cardiovascular events and cardiovascular/total mortality in patients with high blood cholesterol levels and coronary artery disease (CAD). The West of Scotland Coronary Prevention Study (WOSCOPS) further supported efficacy of statins in patients with high blood cholesterol levels, without the incidence of coronary artery diseases. A linear relationship is stated between a reduction in risk of major cardiovascular events and LDL levels of secondary prevention studies with patients undergoing statin therapy (Cannon, et al., 2004). An even stronger linear relationship is observed between LDL levels and course of the atherosclerosis disease with respect to time (Ballantyne, et al., 2008).

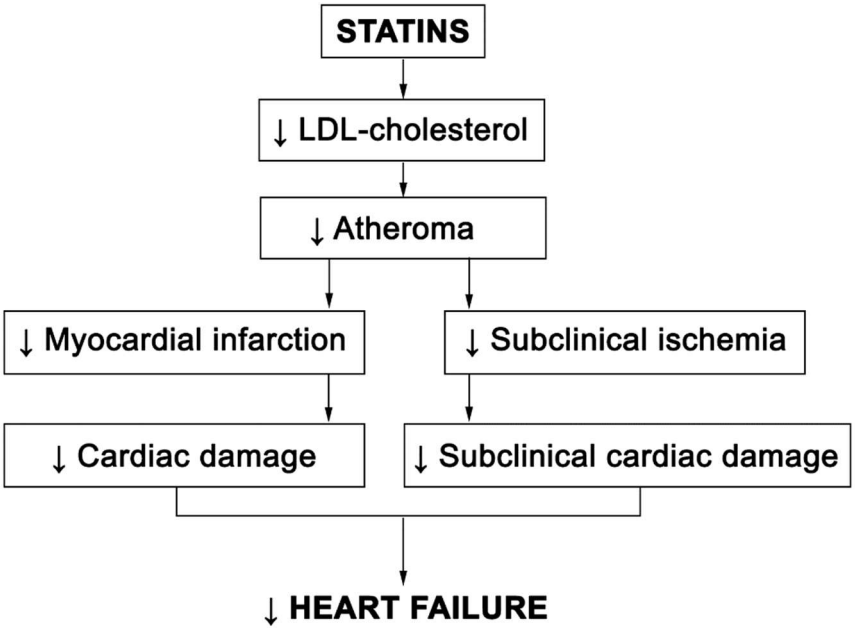

Figure 8. Mechanistic pathways in reduction of heart failure due to statin treatment

Studies show that patients undergoing intensive statin therapy, particularly pravastatin and atorvastatin, showed a reduction in risk in myocardial infarction, cardiac arrest and recurrent ischemia of 16% compared with a use of placebo (Schwartz, et al., 2001). Superior efficacy of intensive statin therapy compared to standard therapy in reducing clinical events in patients with a history of acute coronary syndrome was observed in the IMPROVE IT trial (Ray, et al., 2005). Further studies suggest intensive statin therapy improves survival rates and reduces the progression rate of atherosclerosis (Nissen, et al., 2004). A meta-analysis indicated an overall reduction in major adverse cardiac events and myocardial necrosis in patients undergoing statin pre-treatment with stable angina (Ebrahimi, et al., 2008).

Table 7. Time required for observable benefits in LDL lowering treatment with placebo control (Oesterle et al., 2017)

Statins	Trial name	Patient Group	Time required for observable benefits
Rosuvastatin	JUPITER (Ridker, et al., 2008)	• Elevated hs-CRP (＞2 mg/L) • Without CAD	1.9 years
Atorvastatin	ASCOT-LLA (Sever, et al., 2005)	• Average or lower cholesterol levels • Hypertensive patients	3.3 years
Pravastatin	LIPID (Long-Term Intervention with Pravastatin in Ischaemic Disease	• Broad cholesterol levels • With CAD	6.1 years

	(LIPID) Study Group, 1998)		
	CARE (Sacks, et al., 1996)	• Average cholesterol levels • Myocardial infarction	5.0 years
	WOSCOPS (Shepherd, et al., 1995)	• Men with hypercholesterolaemia • Without CAD	5.0 years
Simvastatin	HPS (Heart Protection Study Collaborative Group, 2002)		2.0 years
	4S (Scandinavian Simvastatin Survival Study Group, 1994)	• High blood cholesterol levels • With CAD	5.4 years
Fluvastatin	LIPS (Serruys, et al., 2002)		3.9 years
Lovastatin	AFCAPS (AFCAPS/TexCAPS Research Group, 1998)	• Average cholesterol levels • Without CAD	5.2 years
Non-statins			
Ezetimibe & Simvastatin (40 mg)	IMPROVE-IT (Cannon, et al., 2004)	• Patients with previous acute coronary syndrome	7.0 years

The efficacy of statins are still in question for patients with chronic renal insufficiency or undertaking renal replacement therapy. In the AURORA study, no significant effects in LDL levels, myocardial infarction and non-fatal stroke were observed with patients being treated with rosuvastatin and simultaneously undergoing haemodialysis. There are only a few studies that address the efficacy of statin therapy for patients with both coronary artery disease and renal insufficiency. Therefore, it can be criticized whether statins are effective for patients with advanced chronic diseases including heart failure and chronic renal insufficiency. Larger prospective studies are required to elucidate this issue.

Although statin treatment is generally regarded as safe, rhabdomyolysis is considered as a risk in the population taking statins (Graham, et al., 2004). Studies have exhibited that statin therapy has a higher incidence of induced rhabdomyolysis when taken conjointly with drugs that alter the cytochrome P450 3A4 system. Atorvastatin, lovastatin and simvastatin are metabolised through the CYP 3A4 isoenzyme system, thus are susceptible to these drug interactions when administered concomitantly.

Table 8. Potent inhibitor substances of CYP 3A4 (FDA, 2010)

Nicotonic acid	Clarithromycin
Macrolide antibiotics	Erythromycin
Cyclosporine	Protease inhibitors • Ritonavir • Saquinavir • Amprenavir • Lopinavir • Nelfinavir
Fibrate	Fluconazole
Delavirdine	Ketoconazole
Grapefruit juice	Nefazodone

In vitro and in vivo data suggest that rosuvastatin is not influenced by the CYP 3A4 isoenzyme system to a clinically significant extent and have further been verified with co-administration with known inhibitors such as fibrate, erythromycin, ketoconazole, cyclosporine and itraconazole. Co-administration of ketoconazole, fibrate and cyclosporine with rosuvastatin showed no change in plasma concentrations, whilst changes observed in itraconazole, fluconazole was not considered to be clinically significant. Drugs that are known to inhibit metabolism via the cytochrome P450 2C9 system, should not be taken concomitantly with rosuvastatin and fluvastatin.

Table 9. Drugs that inhibit metabolism via CYP 2C9 (FDA, 2010)

Amiodarone	Fluvoxamine
Zafirlukast	Azole antifungals
Metronidazole	Cimetidine
Fluoxetine	TMP/SMX
Omrprazole	

In a TNT study, hepatic toxicity in patients undertaking 10mg of atorvastatin was retrieved as 0.2% and in 1.2% of those undertaking an 80mg course. The incidence rate of hepatic toxicity should be less than 1%, which means that patients can produce elevated liver enzymes. In real clinical practice, statins should be prescribed to patients with coronary artery disease and other related cardiovascular diseases, unless they show complications of elevated liver enzymes or rhabdomyolysis.

6.8 Statins and Lactobacillus Strains

Gut microbiome modulation is a novel strategy that has been deliberated for the possible

treatment and prevention of cardiovascular diseases (CVD) with the assistance of statin therapy. The role of the gut microbiome in CVD is a newly emerging field of study, and the bi-directional influences of probiotics and the statin drug is yet to be established. However, modulation of the gut microbiota through a probiotic strategy may generate positive effects in patients with CVD or potentially at risk of CVD, when consumed prior to or concomitantly with statin drugs. The objective is to mechanistically correct microbiota composition, enhancing gut barrier function and modulation of the immune system with the aim to reverse dysbiosis in the microbiota.

Increasing evidence suggests that intestinal microbiota influences the development of cardiovascular diseases (CVD). The progression of cardiovascular disease has been identified to be accelerated due to the alterations in the function of intestinal flora and its composition (Zhou, et al., 2020). The emerging data that is indicative of the bi-directional relationship between cardiovascular diseases and the gut microbiome has surfaced after correlations have been established with other diseases such as digestive system diseases, diabetes, obesity and cancers. Only a few collective microbes are present before the birth of infants, and from birth onwards, it is relentlessly stimulated by external sources to increase the variety and number of microorganisms in the intestinal tract to form a dynamic balance present in the gut (Yatsunenko, et al., 2012). Alterations in the gut in terms of quantity of intestinal micro-organisms and the modifications in species prevalence is due to factors such as dietary habits, intestinal infection and environmental factors. This promotes the development of CVD due to incidences of gut dysbiosis, further causing inflammation in the human body and other metabolic disorders.

As previously mentioned, animal studies by Chan et al., established that with the 12-week supplementation of *Lactobacillus rhamnosus* GG and telmisartan, shifts in gut microbiota proportion were observed, and additional reduction in atherosclerotic plaque present in an atherosclerotic mice model (subjected to a high-fat diet). Five other bacterial species including Eubacteria, Anaeroplasma, Dehalobacteria, Oscillospira and Roseburia have exhibited effective results in prevention of atherosclerosis. Pedro et al., analysed the role of altering gut microbiota in a western diet that is typically representative through high salt consumption in murine models. Result have indicated that aggravation of colitis induced by a high salt diet, reduced the prevalence of *Lactobacillus sp*. This is hypothesised to be due to the alteration in gut immune homeostasis as the inflammatory insults had prompted an increase in vulnerability (Miranda, et al., 2018). Lew et al., observed that *Lactobacillus plantarum* was able to exert cholesterol lowering properties in cells HT-29 and HepG2 along the AMPK pathway, explicitly via phosphorylation of the 5' adenosine monophosphate-activated protein kinase (AMPK), an enzyme that controls fatty acid uptake and glucose activation, hence playing a part in cellular energy homeostasis. This has also resulted in a down-regulated expression of mRNA of HMG-CoA reductase, similar to the behaviour exhibited by metformin. *Lactobacillus plantarum* demonstrated higher cholesterol assimilation ability compared other strains of lactobacilli such as *Lactobacillus reuteri*, *Lactobacillus casei* and *Lactobacillus fermentum*. Another study where supplementation of *Lactobacillus plantarum* probiotic strains for a 12-week period revealed

that hypercholesterolaemic patients had increased levels of HDL and lowered levels of LDL, triglycerides, TC, oxidized LDL and LDL/HDL ratio, revealing that probiotics are effective in hypercholesteremic therapy.

Table 10 examines the effects of Lactobacillus genus probiotics on subjects with CVD risk factors through defined comorbidities such as type 2 diabetes, overweight, obesity, high cholesterol levels and hypertension. Consensus of results demonstrate that probiotics positively affect subjects, by improving Haemoglobin A1c, plasma glucose, LDL and total cholesterol levels after intake.

Table 10. Effect of Lactobacillus genus on subjects with CVD risk factors

Study details	Sample & Treatment	Study design	Results
• Abbasi et al., 2018 (Abbasi, et al., 2018) • Iran	• Sex not mentioned • 44 participants • Overweight • Lactobacillus plantarum A7 strain • Dose: 2×10^7 CFU/g	• Measurement: LDL-cholesterol, triglycerides • Group 1: Probiotic soymilk with *Lactobacillus plantarum* A7 strain Group 2: Conventional soymilk	• Probiotic soymilk consumption showed improved levels of LDL and serum triglycerides when compared with conventional soymlk
• Asemi et al., 2013 (Asemi, et al., 2013) • Iran	• 18 males, 36 females • 54 participants • Type 2 Diabetes • Capsule with probiotic mixture • Dose: 9.52×10^{10} CFU/g	• Measurement: Haemoglobin A1c, total cholesterol, triglycerides, BMI • Group 1: Capsule mixture of: *L. acidophilus, L. casei, L. rhamnosus, L. bulgaricus, B. breve, B. longum, Streptococcus thermophilus* Group 2: Placebo capsule	• Probiotic supplemental consumption prevented rises in the plasma glucose regulation
• Rezaei et al., 2017 (Rezaei, et al., 2017) • Iran	• 44 males, 46 females • 90 participants • Type 2 diabetes • *L. acidophilus La5, B. lactis Bb12* • 2.22×10^9 CFU/g	• Measurement: Systolic blood pressure, vitamin D binding protein (DBP) levels, Fasting blood sugar levels, total cholesterol, triglycerides, Haemoglobin A1c • Group 1: Yoghurt with *L. acidophilus La5, B. lactis Bb12* Group 2: Placebo yoghurt with starter cultures: *S. thermophilus, L. bulgaricus*	• Probiotic yoghurt with *L. acidophilus* showed significant decrease in LDL, triglycerides, plasma glucose and Haemoglobin A1c levels
• Mizushima et al., 2004 (Mizushima, et al., 2004) • Japan	• 46 male participants • Hypertension • L. helveticus or S. cerevisiae • Dose: *L. helveticus:* 7×10^{11} CFU/g *S. cerevisiae:* 2.4×10^9 CFU/g	• Measurement: Systolic blood pressure, vitamin D binding protein (DBP) levels, total cholesterol, triglycerides, • Group 1: Milk containing *L. helveticus* Group 2: *S. cerevisiae* Group 3: Placebo milk	• Probiotic milks had significant decreases in vitamin D binding protein No major changes in TC levels between both milks
• Madjd et al., 2016 (Madjd, et al., 2016) • Iran	• 89 male participants • Obesity • Yoghurt containing: *L. acidophilus LA5, L. bulgaricus, S. thermophiles, B. lactis BB12*	• Measurement: Fasting blood sugar levels, total cholesterol, triglycerides, Haemoglobin A1c • Group 1: Yoghurt containing*: L. acidophilus LA5, L. bulgaricus, S.* Group 2: Placebo milk containing *L. bulgaricus, S.*	• Probiotic yoghurt had decreased LDL and total cholesterol levels • No observed differences in plasma glucose

	Dose: Probiotic yoghurt mixture 1×10^7 CFU/g	*thermophiles* Hypo energetic diet	
• Jones et al., 2016 (Jones, et al., 2012) • Czech Republic	• 41 males, 72 females • 113 participants • High Cholesterol • Yoghurt containing: *L. reuteri* Dose: Probiotic yoghurt 5×10^9 CFU/g	• Measurement: Cholesterol levels, triglycerides • Group 1: Yoghurt containing: *L. reuteri* Group 2: Placebo yoghurt	• Probiotic yoghurt had significantly decreased LDL and total cholesterol levels

The *Lactobacillus* species are a commensal flora and the largest genus members of the lactic acid bacteria (LAB), which is defined generally as a group that is characterized by lactic acid formation acting as the main end product of carbohydrate metabolism (Walter, 2008). The *Lactobacillus* group is present in the human gastrointestinal tract, mouth and the female genitourinary tract. The genus *Lactobacillus* is an established genus utilized as probiotics, with a history of a safe use and recognised as safe (GRAS) by the US Food and Drug Administration for application in nutritional powers, dairy products and functional beverages. It is reported that probiotics in the *Lactobacillus* genus can regulate the enzymes NPC1L1, ABDG8 and ABCG5 that are liable for cholesterol transport within the intestinal gut, and enzymes like HMGCR and LDLR which are responsible for homeostasis and regulation of cholesterol in the liver. The primary approach in controlling the *de novo* synthesis of cholesterol levels is by the regulation of HMGCR activity.

The types of microenvironmental cues of the gut can be biochemical, physio-chemical and mechano-structural. Major factors present in the microenvironment are oxygen, pH, nutrients, flow and topography. Each strain has inherent sensitivities with each factor, thus reside in precise regions of the gut. The first step in comprehension in the behaviour of bacterial strains with its' microenvironment is to indicate the oxygen uptake and consequently the oxygen gradients between each defined growth regions of the gut. This ties in with the research that has been conducted in Semester 1, 2020, whereby a hydrogel bioreactor was proposed with gradient structures to mimic pH and oxygen maintenance that is sustained in the human gut. The initial scope of this project was to prepare a physical model bioreactor using the growth parameters gathered to investigate permeability and diffusion, and consequently optimizing and validating this knowledge to produce a feasible gut model that is able to grow multiple tuneable strains of aerobic and anaerobic strains. However, due to the COVID-19 pandemic, this method was not possible. Hence, a theoretical approach is determined by computer modelling to take the first steps in human gut biomimicry and finding feasible and efficient methods in probiotic strain growth.

The bacterial strain *Lactobacillus delbrueckii* subsp. *bulgaricus* will be chosen to monitor its modulation of the gut in order to understand the behaviour these strains have with the microenvironment. The *Lactobacillus delbrueckii* subsp. *bulgaricus* is a homofermentative lactic acid bacteria, that is the main bacterium used in yoghurt production and cheese ripening. Optimal growth is observed in the temperature range of 40-44 °C under anaerobic conditions. This bacteria within the hydrogel bioreactor will be modelled accordingly by its

oxygen consumption as research suggests direct correlation with its' growth curves (Hao, et al., 2011).

Probiotic Phylum	Probiotic species	Gram +/-	Type	Aerobic/ Anaerobic	pH tolerance range	Other
Firmicutes	L. delbrueckii Subspecies: *L. d.* subsp. *bulgaricus*	+	Rod, long and filamentous	Anaerobic	4.6-5.4	Non-pathogenic

6.9 Importance of gut microbiome modelling

The human gut microbiome is a diverse and complex ecosystem, comprising of up to 10^{13} – 10^{14} microorganisms (Martin, et al., 2014). The precise compositions of the bacterial communities within the gut microbiota is dependent on environmental factors (dietary habits, drugs and microbial inocula), secretory products, host genotype and peristalsis (Egert, et al., 2006). It has been established that host diet plays a major role in microbial composition. Therefore, an analysis on patients at risk of cardiovascular diseases undertaking rosuvastatin therapy was selected to focus on patient grouping for more effective management and understanding of the bi-directional interactions of the microbiome and statin drug.

Due to the high variability in the composition of gut microbiota within the human population and incomplete data makes it difficult to produce fully deterministic modelling in the human gut microbiome. Further patient classification should be made for accurate prognosis such as diagnosis related groups (DRG), age group, country and sex. However, due to absence of literature available in these specificities, an overview was completed by addressing valuable relationships that may be of help in future research. Computational modelling will play a major role in interpretating experimental data and forecasting responses for dietary modulation.

Current methods of studying the ecosystem provides a relatively restricted insight into the function of the gut microbiota which includes approaches such as spectrometry-based analyses, metagenomics, microfluidics, culturomics and metatranscriptomics. The interaction between species is rarely demonstrated and seldom gives understanding into individual or community-level metabolic functions. Several modelling systems have been employed to gain useful insight into how human health and disease are impacted by gut microbiota, but further research is required to produce robust models that incorporate multi-dimensional behaviours. Computational modelling will assist in the simulation of the bi-directional interactions of the statin drug with use of probiotics, in a non-invasive manner that will prove higher accuracy and be more valuable in gaining a comprehensive understanding than in-vitro studies that are available.

Research that has been explored in the Feasibility Report in Semester 1, 2020 has substantiated the significance in understanding the microbiome to assist in human health and disease. By understanding how to manipulate the properties in the microbiome, designing tailored solutions would also be possible. Bacterial strain growth in the modelled gut bioreactor had also been explored as a feasible method in reducing probiotic costs. The clinical efficacy of probiotic use has been an expansively researched mode of biotherapeutics; however comprehensive claims in studies have occasionally presented contrasting results which has led to ambiguous and conflicting overall conclusions by professionals in the medical field. Probiotic formulation with taking factors such as ethnicity, sex, age and geographical locations into account will increase the efficacy of the probiotic product compared to the typical supplier's solution of "one size fits all" model.

Due to a high degree of functional redundancy, simplifying the gut microbiome will assist in producing a feasible and desirable system that addresses dynamics and functional interactions in a quantifiable manner. Computational methods will help guide in developing the proposed hydrogel bioreactor and maintain pH and oxygen gradients as sustained in the gut in the future.

7. Model Methodology / Design and Justification

7.1 Project management

Upon establishing the rationale for modelling this project, an initial plan was drawn up to manage the project. This project was to be iteratively built up instead of attempting to build everything at once for ease of project management. The Gantt chart that guided the modelling section of this report can be found in Appendix 10.2.

For this project, the chosen software had to balance a number of needs. It had to be suitable for prototyping scientific data, have the correct libraries for the product, and be able to show complex surface plots. It had to be accessible to all students and supervisors with supervisors having a level of expertise in the software to teach students. For the above reasons, MATLAB was chosen. MATLAB is operating program independent, extremely fast and is known for its plotting and modelling capabilities in industry. (Cooperative Institute for Meterological Satellite Studies, 2000)

The first stage of the system was to characterise the diffusion of oxygen through the layers of the in-situ fibrous bed reactor.

The key term of this system is the change of oxygen over time as the reactor is exposed to the surrounding air in a controlled fashion. Like many natural phenomena, the state of oxygen in the system is reliant on the state of itself at all points throughout the reactor over time.

The system can therefore be well approximated by the use of a parabolic partial differential equation as it is time-dependent and can be calculated by the imposed relationship between the concentration of available oxygen, the diffusion of the oxygen through the hydrogels.

7.2 Preliminary approach and results

For a Cartesian one-dimensional system, the concentration of the oxygen throughout the reactor, **C**, at location **x** and time **t** can be shown with the following parabolic partial differentiation equation:

$$\frac{\partial \mathrm{C}(\mathrm{x},\mathrm{t})}{\partial \mathrm{t}} = \nabla \cdot [\mathrm{D}(\mathrm{C},\mathrm{x})\nabla \mathrm{C}(x,\mathrm{t})]$$

Where **D(C,r)** is the diffusion coefficient at each point throughout the reactor. The flux of the material at any part of the system is proportional to the local concentration gradient. We assume that the diffusion coefficient changes at a small enough rate to be functionally constant throughout each hydrogel. No material is created or destroyed in this process.

The linear diffusion equation can be displayed in the same form as the heat equation, allowing for the adaption of heat flux experiments and literature to this project.

$$\frac{\partial \mathrm{C}}{\partial \mathrm{t}} = D\nabla^2 C = 0$$

In a cylindrical coordinate system (ρ, ϕ, z) at steady state $\left(\frac{\partial \mathrm{C}}{\partial \mathrm{t}} = 0\right)$ we further assume that C uniformly distributes along ϕ and z directions.

$$\frac{1}{\rho} \times \frac{\partial}{\partial \rho}\left(\rho \frac{\partial \phi}{\partial \rho}\right) + \frac{1}{\rho^2} \frac{\partial^2 \phi}{\partial \phi^2} + \frac{\partial^2 \phi}{\partial z^2} = 0$$

The project was first modelled using the partial differential solver in MATLAB, pdepe. The partial differential solver solves systems of parabolic or elliptic PDEs for a function $u(x,t)$ in the form:

$$c\left(x,t,u,\frac{\partial u}{\partial x}\right)\frac{\partial u}{\partial t} = x^{-m}\frac{\partial}{\partial x}\left(x^m f\left(x,t,u,\frac{\partial u}{\partial x}\right)\right) + s\left(x,t,u,\frac{\partial u}{\partial x}\right)$$

Where

$$f\left(x,t,u,\frac{\partial u}{\partial x}\right) \text{ is a flux term}$$

$$s\left(x,t,u,\frac{\partial u}{\partial x}\right) \text{ is a source term}$$

$$c\left(x,t,u,\frac{\partial u}{\partial x}\right)\frac{\partial u}{\partial t} \text{ is a scaling term}$$

m is a dimensionality term and can be $0, 1$ or 2 depending on whether the system is in slab, cylindrical or spherical coordinates. Setting m to any of these integers automatically sets the dimensionality of the system. (MATLAB, 2020) The code can be found in Appendix 10.3

The results showing time, concentration and coordinate in the reactor can be seen in Figure 10**Error! Reference source not found.**. A clearer side profile of the reactor, showing the oxygen penetration at $t \approx 11$ hours can be found in Figure 9 where the superior accuracy of

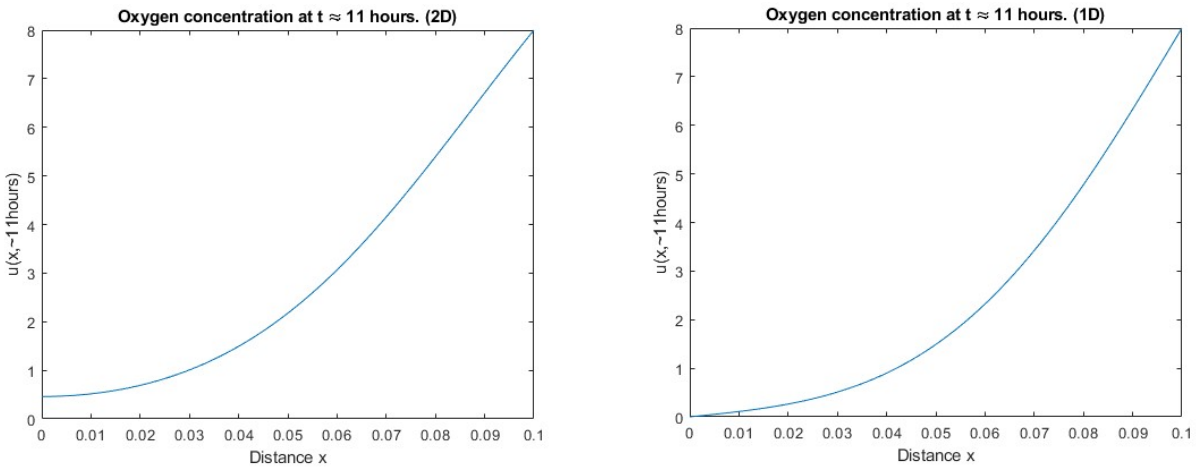

Figure 9 Side profiles of the oxygen concentration throughout the reactor at approximately 11 hours

the oxygen diffusion can be seen, accurately showing the slight but extant oxygen concentration in the centre of the reactors. The diffusivity of cellulose was sourced from (Hulst, et al., 1989).

The partial differential solver has no inbuilt functionality to solve for a system of interdependent equations, rather analytically solving one equation in a stepwise fashion. A workaround was attempted by implementing a for-loop to iteratively solve each hydrogel over the time of the experiment. The system would be iteratively solved by looping through

each hydrogel and solving at each point, with each output returned as an input to the next hydrogel.

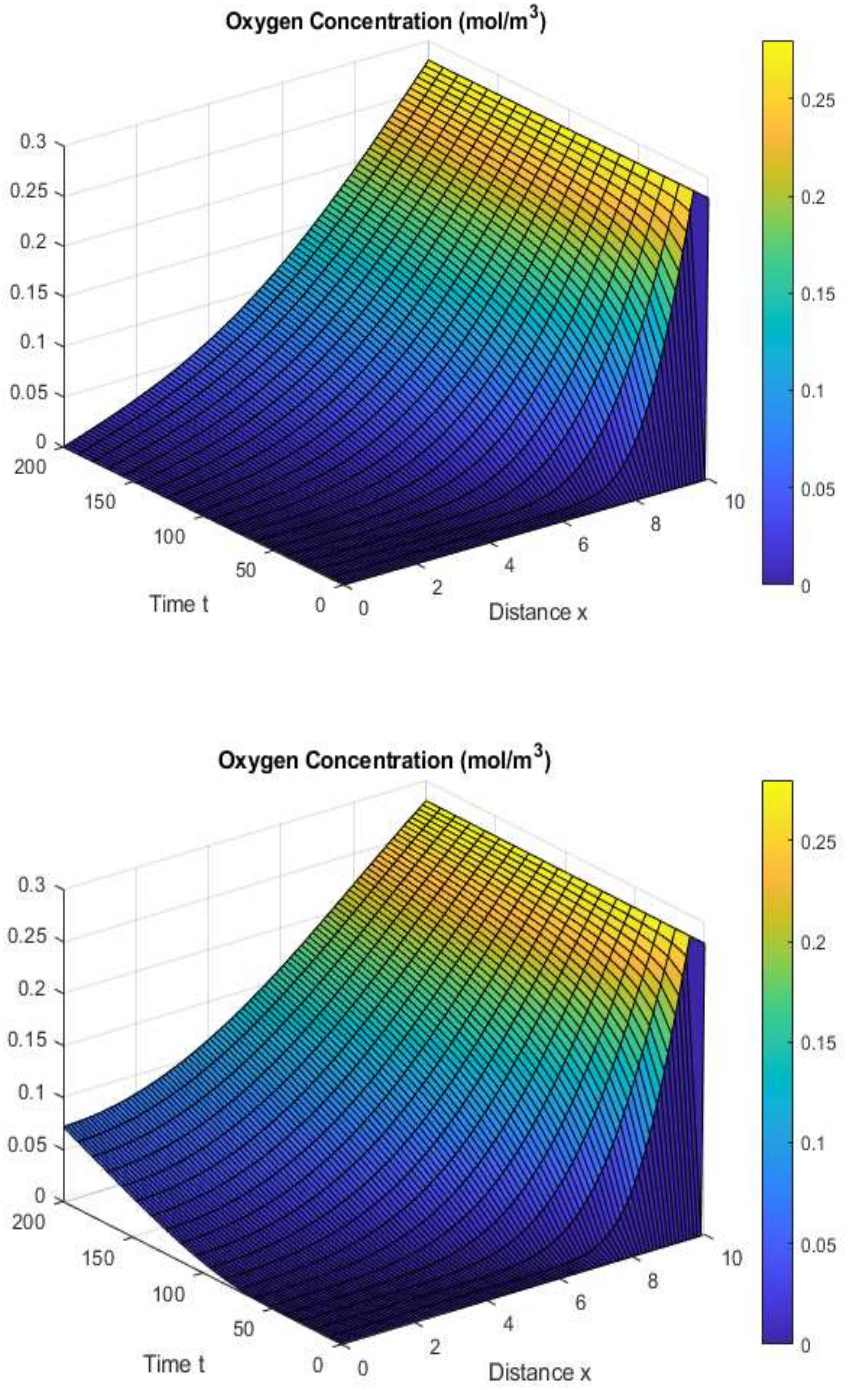

Figure 10 Figure 10 A 1-D (top) and 2-D (bottom) model showing oxygen concentration over the reactor over time. Time is shown in minutes and distance is shown in centimetres where the centre of the reactor can be found at x=10. Note the non-zero end-result of the cylindrical model at t=end, signifying the full penetration of oxygen through the hydrogel bed.

For added customisation an array that stores the different bulk moduli of the hydrogel was created and populated with values sourced from academic research. Each of those values would then be called in an iterative fashion into the required hydrogel, as the simulation

stepped through each for-loop to produce an initial model that controlled for bulk moduli through the system, albeit with loss of accuracy at hydrogel interface points.

This however proved to be cumbersome and slow and a new solution was pursued.

7.3 Refined approach

The long computational time and inflexibility of MATLAB's partial differential solver for separate systems of partial differential equations had rendered it unsuitable to expand and a new numerical analysis has been adapted for this project.

MATLAB's multi-paradigm matrix manipulations, data plotting and algorithm implementation allowed for the rapid adaption of the Crank-Nicholson finite difference method as an alternate means of calculation. (Sweilam, et al., 2012) The Crank-Nicholson method is a finite difference method for solving systems of partial differential equations. It has the benefit of being second order accurate and having second order time convergence while enjoying the stability of time implicit methods.

The Crank-Nicholson method is simply the average of the forward time difference to approximate the time and space derivative and the backward time difference that approximates the time derivative. For the generalised diffusion equation, including the source/sink term $O_{consumed}(x,t)$:

$$\frac{\partial \mathrm{C}}{\partial \mathrm{t}} = D\frac{\partial^2 \mathrm{C(x,t)}}{\partial \mathrm{x}^2} + O_{consumed}(x,t)$$

Where the term $O_{consumed}(x,t)$ is a measure of net oxygen consumption (or generation) by aerobes in the reactor. Oxygen is the key variable of consideration for the reactor with further chemical species planned for a future iteration of the project.

For a given spatial location of the finite volume j at time n, the forward difference scheme to approximate the time derivative is given simply as the difference of concentration at each of these points in time and space averaged over time. Going forward from time n:

$$\frac{C_j^{n+1} - C_j^n}{\Delta t}$$

Where this time derivative is equal to an approximation of the second space derivative that centred at j at time n.

$$\frac{C_j^{n+1} - C_j^n}{\Delta t} = D\frac{C_j^{n+1} - 2C_j^n + T_{j-1}^n}{(\Delta x)^2} + O_j^n$$

The backward time centred scheme that approximates the time derivative at time $n+1$ and how it relates to the approximate second space derivative is:

$$\frac{C_j^{n+1} - C_j^n}{\Delta t} = D\frac{C_{j+1}^{n+1} - 2C_j^{n+1} + T_{j-1}^{n+1}}{(\Delta x)^2} + O_j^{n+1}$$

The Crank-Nicholson method averages the two to yield a more accurate equation. The new concentrations can then be put in terms of the old concentrations to yield a tridiagonal matrix that can be used to solve for all required points.

$$CN = \frac{C_j^{n+1} - C_j^n}{\Delta t} = \frac{1}{2}\left(D\frac{C_j^{n+1} - 2C_j^n + T_{j-1}^n}{(\Delta x)^2} + O_j^n + D\frac{C_j^{n+1} - 2C_j^n + T_{j-1}^n}{(\Delta x)^2} + O_j^n \right)$$

The stencil for all three methods is shown for reference in Figure 11.

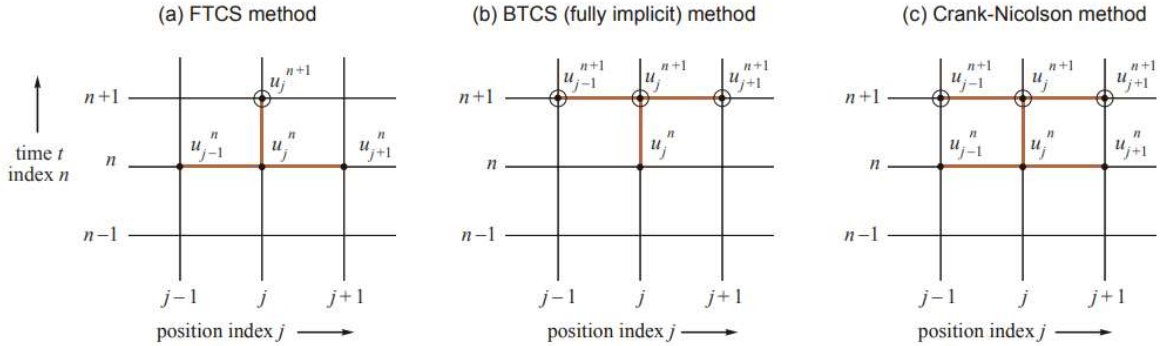

Figure 11 Numerical analysis stencil for the Forward Time Centred Space method, the Backward Time Centred Space method and the hybrid Crank Nicholson method.

The Crank Nicholson method showed immediate advantages over the partial differential equation solver. The code was generated both with and without the implementation of indexes representing the layers.

In the initial attempt, the Crank-Nicholson matrix to be solved was generated over a period of 40 hours and 1000 time-steps. The tri-diagonal matrix was iteratively built up using for-loops to set up the upper, middle and lower element (Figure 12). This can be found in Appendix 10.4.

A new approach was created to discretely account for the unique environment at each layer. 10 equally spaced interfaces were initially set up to model the stratified hydrogel layers. It is assumed that all interfaces had perfect contact throughout the reactor.

The code was improved upon by implementing an upwind scheme to discretise the system of partial differential equations to simulate the propagation of oxygen through the reactor. (Fitzpatrick, 2006)

$$\begin{bmatrix} 1 & 0 & 0 & 0 & 0 \\ -\frac{\alpha}{2} & 1+\alpha & -\frac{\alpha}{2} & 0 & 0 \\ 0 & -\frac{\alpha}{2} & 1+\alpha & -\frac{\alpha}{2} & 0 \\ 0 & 0 & -\frac{\alpha}{2} & 1+\alpha & -\frac{\alpha}{2} \\ 0 & 0 & 0 & 0 & 1 \end{bmatrix} \begin{bmatrix} T_0^{n+1} \\ T_1^{n+1} \\ T_2^{n+1} \\ T_3^{n+1} \\ T_4^{n+1} \end{bmatrix} = \begin{bmatrix} a \\ R_1^n \\ R_2^n \\ R_3^n \\ b \end{bmatrix}$$

Figure 12 The tri-diagonal matrix, showing each new temperature in terms of the old temperature, α, for a given heat equation with the same properties as our diffusion equation. The upper left and lower right points are known as boundary conditions. (Bioh, 1997)

The scheme takes into consideration the spatial differences 'upstream' of the initial boundary condition and uses them to calculate values in the centre of the reactor – i.e., it uses a solution sensitive stencil to numerically simulate the direction

of propagation. It is stable and popular for both parabolic and hyperbolic partial differential equations – especially those with rough wave forms.

In the MATLAB model, its implementation is given as a special spatial step h to keep the Crank-Nicholson model stable:

$$\frac{dC}{dr} = \frac{1}{2} \times \left(C_{i+1}^{n+1} - \frac{C_i^{n+1}}{h} + C_{i+1}^{n} - \frac{C_i^{n}}{h} \right)$$

Where:

$$dt = t^{n+1} - t^{n}$$

$$\frac{dC}{dt} = C_{i+1}^{n+1} - C_i^{n+1}$$

More details on its full implementation can be found in Appendix 10.5.

7.4 Introducing a consumptive oxygen term

There is a dearth of data that describes oxygen consumption of a probiotic system over time due to the many extenuating factors that affect growth. A small body of research has been conducted into oxygen consumption of common bacteria in the first half of the 20th century which shines light on this research and provides a means of measuring bacterial oxygen consumption at laboratory conditions. (Martin, 1932) (Johnson, 1936). Martin's method of establishing the oxygen consumption of *Escherichia coli* was fundamental to the calculation of oxygen consumption of an obligative aerobe and its oxygen consumption in the reactor.

While *E. coli* itself is part of the normal microbiota of the human gut, benefiting its hosts by producing vitamin K (Meganathan & Kwon, 2009), the data generated from Martin was not considered for direct use as a priority. An obligative aerobe was required to produce a more reliable benchmark of aerobic growth. This in contrast to the facultative anerobic capabilities of *E. coli*, which may skew growth rates and thus oxygen consumption in the anaerobic core of the fibrous bed reactor.

Probiotic choice was assisted by the catalogue of probiotics and their properties generated in the first semester's progress report. Lack of data available for purely obligative aerobes resulted in *L. Bulgaricus* PTCC1737 being selected for its relatively low ability to facultatively perform as an anaerobe. (Rezvani, et al., 2017)

Drawing data from (Kolbeck, et al., 2019) the consumption rate of oxygen per cell per hour *Brochothrix thermosphacta* was found to be 0.748 pg. *B. thermosphacta* is a spoilage bacterium closely related to *Lactobacillus* bacterium. It has similar facultative anaerobic capabilities as *L. bulgaricus* and is a good candidate for oxygen data.

The oxygen uptake rate for *B. thermosphacta* falls within the same magnitude as Martin's findings for *E. coli*, thus adding to its validity given the similarity in energy requirements of this bacteria and *E. coli* in an oxygenated environment. As the central purpose of the modelling is provide the structure of the model, more accurate experimentally derived data may be included later.

Growth data over time for *L. bulgaricus* were adapted from (Rezvani, et al., 2017). Data from (Martin, 1932) (Davis, 2014) was used to convert from grams to colony forming units and an integral was generated to provide the oxygen consumption of *L. Bulgaricus* per cell over time, factoring in the lag, log and stationary growth phase of the bacteria.

$$\int_{t_{start}}^{t_{end}} \frac{f(cell\ growth\ in\ g)}{t} \times \frac{10^{-12}(CFU)}{g} \times \frac{oxygen\ uptake}{CFU \times t} dt$$

With the purpose of the function to get total growth as opposed to a squared rate. A sigmoidal fit of the data was determined using MATLAB's data fitting tool to remove the residuals in the resultant solution. A data fit was necessary as cell growth data for *L. bulgaricus* was only available for limited periods.

The raw cell growth data over time is given in

time (h)	**0**	**6**	**12**	**18**	**24**	**30**	**36**	**42**	**48**	**52**
Cell dry weight (g)	0	0.2	0.9	2.5	4.2	5.1	5.1	5	5.1	5.2

Table 11 and the sigmoidal fit of the data is shown in Figure 13**Error! Reference source not found.**.

time (h)	**0**	**6**	**12**	**18**	**24**	**30**	**36**	**42**	**48**	**52**
Cell dry weight (g)	0	0.2	0.9	2.5	4.2	5.1	5.1	5	5.1	5.2

Table 11 Raw cell growth data for L. Bulgaricus (Rezvani, et al., 2017)

The sigmoidal fit in Figure 13**Error! Reference source not found.** is in form:

$$f(x) = \frac{5}{1 + a \times e^{-bx}}$$

Where coefficients with 95% confidence bounds are:

$$a = 148.5\ (12.64, 284.3)$$

$$b = 0.2805\ (0.2304, 0.3305)$$

With the goodness of fit being:

$$SSE = 0.1493$$

$$R^2 = 0.9966$$

$$Adjusted\ R^2 = 0.9962$$

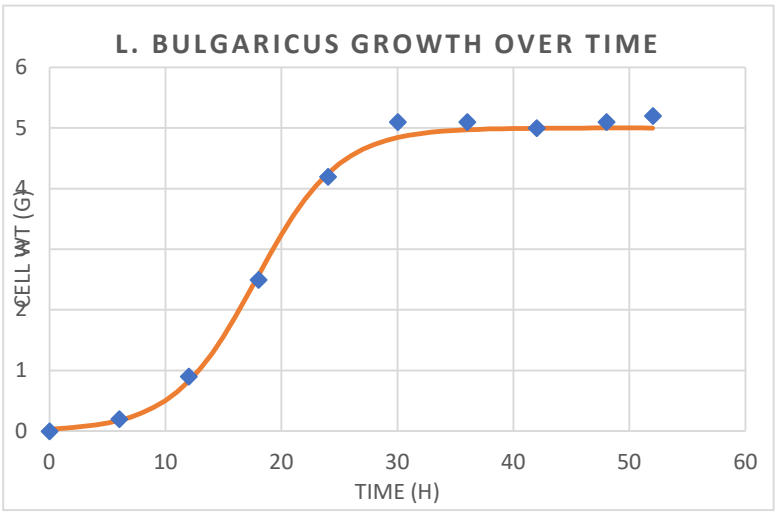

Figure 13 L. Bulgaricus growth – sigmoidal fit.

Inserting this data into the new upwind scheme code as a function and modifying it accordingly, one can see the impact of oxygen consumption over time (Figure 14) and without the probiotic species (Figure 15) with the slightly flattened curves of each hydrogel's oxygen diffusion over time.

The diffusion curves are only marginally flattened due to the low consumption of oxygen relative to the constantly dissolving oxygen on the side at which the fibrous-bed reactor is exposed to the air, thereby demonstrating its efficacy for use for aerobes and facultative anaerobes at each strata.

Both Figure 14 and Figure 15 show the varying hydrogels across the full extent of the reactor rather than each hydrogel over each concentric area of the in-situ fibrous-bed reactor. This schema was chosen to better display the oxygen diffusion curve for each hydrogel over time than have them be influenced by previous hydrogel diffusivity. This set-up allows researchers to make a more informed choice of how to order hydrogels and bacterial inoculation for optimal hydrogel placement. The structure of the code allows for the hydrogel layers and properties to be switched around per researchers' will.

A full copy of the code can be found in the appendices. Along with the hydrogel placement and permeability, the code allows the user to modify the oxygen consumption and with that the aerobic cell growth concentration. Only the data for the oxygen consumption of *L Bulgaricus* has been included in each layer of the hydrogel but other oxygen consumption rates can be derived in the same manner as described for *L. Bulgaricus*. This final code can be found in Appendix 10.7.

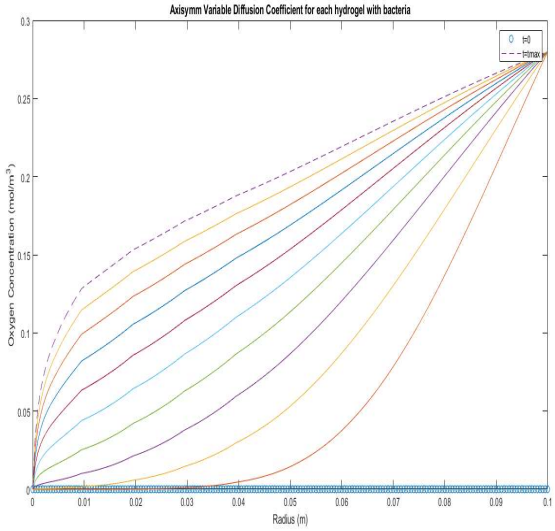

Figure 14 Axisymmetric variable diffusion effect on 10 hydrogels with bacteria

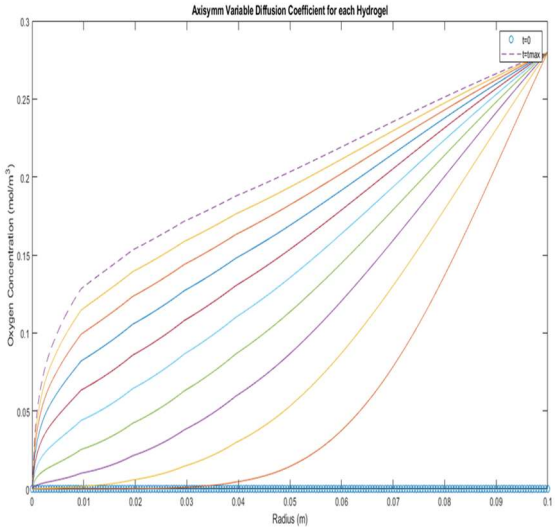

Figure 15 Axisymmetric variable diffusion effect on 10 hydrogels without bacteria

8. Discussion / Recommendations

8.1 Challenges and future work

8.1.2 Data bias

There are intrinsic challenges in converting a multi-dimensional system in which the substituents are so inter-dependent upon one another into a model with only limited interactions. Interaction data is sourced through experiments in set conditions which may not fully resemble the range of the experiment, rather serving as an approximation. Furthermore, this data is only as reliable as the rigor of the experimenter. Both confounding and extraneous variables such as temperature, time of experiment and implicit experimenter bias may all contribute to data being presented in one way or another, and with that influencing the utility of the data. Thankfully, the latter effect can be assumed to be relatively low and of minimal concern. This branch of research is concerned with physical and biological phenomena, the effects are supposed to be significantly less pronounced that if this project was to be conducted on more sociological phenomena – for example, the communal impact of dysbiosis.

These assumptions can be tested by confirming each value against a checklist of the used data to establish accuracy.

8.1.3 Gas diffusion

The flow of oxygen into the reactor is modelled to occur in the same fashion as described by the progress report in semester 1. Namely, through a drilled hole of a set size into the reactor of a given diameter. Upon sealing the reactor and purging the inner layers with nitrogen gas, atmospheric oxygen would be allowed to penetrate the stratified hydrogel layers of the reactor to produce the oxygen gradient shown in Figure 9.

A future addition to this project would be the expansion of the data displayed from cylindrical axisymmetric coordinates to a full 3D structure in a fluid modelling package such as COMSOL®. This would better show the rate of change of oxygen concentration at the areas away from the access and exchange holes (Figure 16). A local concentration oxygen gradient is assumed to exist around this area that cannot fully be captured by a one-dimensional model.

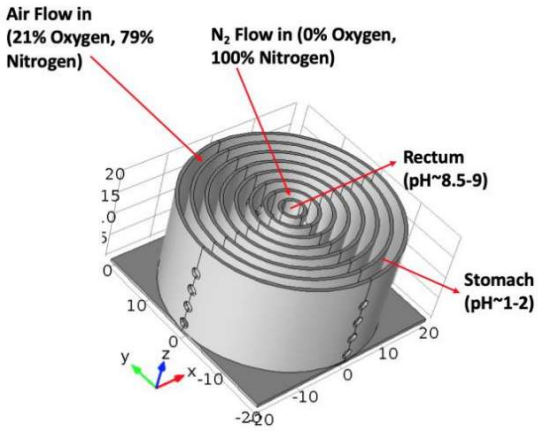

Figure 16 A mock-up of the bio-reactor from the progress report showing access holes, exchange holes, gas flow and pH throughout the reactor.

Additionally, only oxygen flow is included in the model due to its importance. Other atmospheric gases (most notably nitrogen) have not been modelled due to time constraints and relatively low impact on bacterial growth.

Hydrogel interfaces

The occluding effect of the mesh filters as described in the progress report has been left for future work due to the time constraints of this project. The interface between hydrogel

layers are assumed to show perfect adhesion. That is, complete lack of air-bubbles and zero contact roughness due to surface imperfections or the amorphous crystallinity of the utilised bio-medical polymers. (Shah & Vasava, 2019)

Interfaces provide a challenge for modelling mass transport between hydrogels. The fit at interfaces is quasi-random and limited attempts have been made to model their fit. Most efforts in this area have been focused on exploring the interaction between contact lenses and the eye. (Arjmandi & Ramezani, 2019) (Pimenta, et al., 2019) (Stapleton, et al., 2006)

As it stands, perfect hydrogel contact is assumed to occur without the addition of separation meshes. Experimental tests are required to test these effects and the effect of the implementation of separation barriers.

8.1.4 Reactor diffusion

Interface interaction discussed in the previous section ties into the broader limitation that this model's geometry is composed of layers of sandwiched hydrogels which are in contact at set points throughout the reactor. The thickness of each hydrogel layer can have a cascading effect of oxygen flow through the whole reactor. An increase of thickness of a layer, to produce a greater volume for a set hydrogel to grow, will have implications on the oxygen level throughout the rest of the reactor. If the hydrogel of a given strata and a given oxygen permeability coefficient is increased at the expense of a hydrogel in a different layer with a different permeability coefficient, the resulting oxygen diffusion will change. This could have implications on yield for facultative anaerobes deeper in the reactor and further away from the replenishing supply of oxygen at the outer layers.

The challenge remains in how to compensate for these variations. Possibilities include comparing a baseline desired oxygen level to the new oxygen level and calculating how much extra oxygen should be supplemented through pumps.

It remains to be seen if this change would have considerable effects on bacterial growth given that oxygen consumption of aerobes is in the picogram range per CFU. The sheer excess of dissolved oxygen relative to the oxygen consumption of aerobes may very well have no effects on the bacterial growth, even at more anoxic conditions toward the centre. This can be determined experimentally.

9. Conclusions

The influences on the bi-directional interactions of the gut microbiome and the drug rosuvastatin was analysed for patients at risk of cardiovascular diseases. Observations and trends that could be considered upon the animal and human studies that were available:

- Greater composition of the phylum Firmicutes and the genus which falls under it as *Lactobacillus*, as well as *Bifidobacterium* presented better statin response, as patients were able to more effectively achieve normal blood lipid levels, and displayed anti-obesity and anti-diabetic properties
- Additionally, gender has been shown to influence microbial diversity, as do risks of CVD that increases in men
- Higher gut biodiversity was also associated with a statin sensitive response

Trends associated with rosuvastatin's influence on the microbiome:

- Statin therapy is potentially the driving force of gut microbiome alterations, hence escalating dysbiosis in the gut
- Based on in vitro experiments, it has been assumed that statins employ their modulation on gut communities by directly disrupting bacterial membrane architecture. This antimicrobial activity is less in rosuvastatin, compared to simvastatin and atorvastatin.

Studies have shown that the lactobacillus genus has frequently improved LDL or low-density lipoproteins and total cholesterol levels in patients at risk of CVD, as they can regulate enzymes that are liable for cholesterol transport within the gut. Hence, the bacterial strain, *Lactobacillus bulgaricus* was chosen to monitor its modulation of the gut through computational modelling.

Gut microbiome interactions with drugs is a relatively novel approach, Although it can be inferred that the influence of statins in patients had been compromised in the presence of gut dysbiosis, evidence is lacking to provide personalised therapeutic treatments based on their gut microbiome composition. Further research is required to form significant correlations between statin treatment and the gut microbiome.
A model of the in-situ fibrous-bed reactor was successfully created. Oxygen diffusion and aerobic consumption of dissolved oxygen was modelled using the Crank-Nicholson method with an upwind scheme and an added sink term. The model was constructed using MATLAB. It was found that oxygen will penetrate through 0.1m of common hydrogels used in biological applications in as little as two hours.
The introduced facultative anaerobe was found to have little impact on oxygen diffusion due to the relatively high oxygen replenishment from the atmosphere. This work paves the way for extensive experimental work and serves as a framework for further research.

10. Appendix

10.1 Timeline

Statin review	Tina Gunasekara		
Research and choose suitable drug with relevant literature	100%	24/7/20	31/7/20
Finalise chosen drugs and correlating disease	100%	29/7/20	7/8/20
Consider additional medicinal drugs for correlating disease	100%	1/8/20	8/8/20
Preliminary research on statins, particularly rosuvastatin	100%	7/8/20	14/8/20
Research the beneficial cardiovascular effects of statins	100%	14/8/20	21/8/20
Research pleiotropic effects of statins	100%	21/8/20	28/8/20
Research effects of statins on microbiome & biological effects (clinical, basic, animal, studies)	100%	28/8/20	11/9/20
Research statin use for cardiovascular prevention	100%	11/9/20	20/9/20
Research statins and Lactobacillus strains + Epidemiology of CVD	100%	21/9/20	1/10/20
Compile and edit Final Report	100%	1/10/20	11/10/20
Compile and edit professional practice contribution	100%	11/10/20	13/10/20
Submission of final report	100%	13/10/20	17/10/20
Prepare and edit presentation + Poster	100%	13/10/20	16/10/20
Submission of professional practice and contribution	100%	17/10/20	21/10/20
Submission of presentation	100%	16/10/20	19/10/20

10.2. Gantt chart for the modelling section of the report

RMIT University
Grupel, Gunasekara

Project Start: Mon, 7/20/2020
Display Week: 1

TASK	ASSIGNED TO	PROGRESS	START	END
Completion plan	Both			
Meet with professors		100%	25/7/20	25/7/20
Set scope for final project		100%	25/7/20	1/8/20
Discuss roles and tasks		100%	28/7/20	2/8/20
Create a completion plan		100%	20/7/20	9/8/20
Create a plan and gantt chart		100%	3/8/20	9/8/20
Numerical modelling	Tyrone Grupel			
Research initial ideas into COMSOL modelling		100%	26/7/20	30/7/20
Organise individual tasks and completion plan		100%	28/7/20	4/8/20
Get MATLAB equations from QS		100%	4/8/20	6/8/20
Create an initial axisymmetric model of the reactor		100%	30/7/20	20/8/20
Calibrate initial model are Srinivas's comments		100%	6/8/20	20/8/20
Create initial equations to tune for probiotic volume through reactor layer size.		100%	21/8/20	4/9/20
Get equations in correct form that accounts for the multiple layers of hydrogels		100%	28/8/20	18/9/20
Research oxygen consumption term for aerobes in system		100%	11/9/20	14/9/20
Refine oxygen modelling and troubleshoot errors		100%	11/9/20	25/9/20
Compile and edit Final Report		100%	18/9/20	16/10/20
Write up findings		100%	2/10/20	16/10/20
Submission of final report		100%	9/10/20	16/10/20
Prepare and submit presentation & professional practice contribution		100%	16/10/20	18/10/20

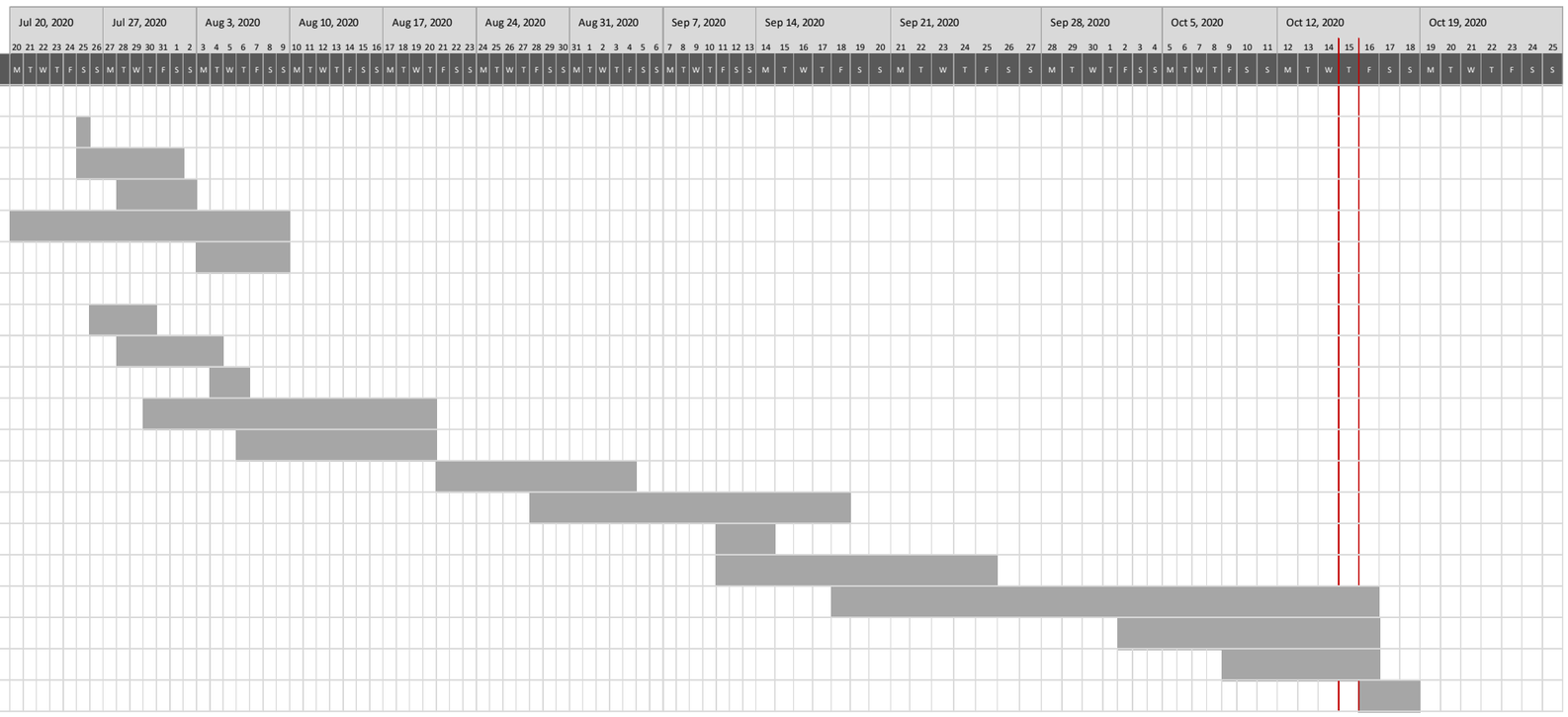

10.3 MATLAB's partial differential solver, one hydrogel.

```
xf=0.1; xdivisions=100; %Outer hydrogel x value and mesh divisions in spatial coordinate
x = linspace(0,xf,xdivisions); %spatial mesh, % 10 cm gel thickness, x in meter
t = linspace(0,40000,40); % Time points for solution calculation, time in seconds
m = 0;
sol = pdepe(m,@pdex1pde,@pdex1ic,@pdex1bc,x,t);
u = sol(:,:,1);
figure
surf(x,t./3600,u) % Convert time to hrs
title('Oxygen Concentration (mol/m^3) (1-D Cartesian coordinates with no symmetry')
xlabel('Distance (m)')
ylabel('Time (h)')

figure;
diff=plot(x,u(end,:));
title('Solutions at t ? 11 hours.(1D)');
xlabel('Distance x');
ylabel('u(x,~11hours)');
%the individual points can be harvested into an xlsx file by running the
%following code:
%diffm=get (diff, 'XData'); diffm=get (diff, 'YData'); writematrix(diffm,'diff1d.xlsx');

% figure
% plot(x,u(end,:),'o',x,exp(-t(end))*sin(pi*x))
% title('Solution at t = 2')
% legend('Numerical, 20 mesh points','Analytical','Location','South')
% xlabel('Distance x')
% ylabel('u(x,2)')

function [c,f,s] = pdex1pde(x,t,u,dudx) % Equation to solve
xf=0.1; % 10 cm gel thickness
%c = 0.8*(1-(1-x/xf)); %Porosity as a function of spatial coordinate
m=0; %axisymmetric
c = 0.8; % Constant Porosity
f = (dudx)*1.79E-8*0.8; %D=1.79E-8; %diffusion coefficient for 3% alginate (Hulst et.al.
1989)
s = 0; % No production/consumption of oxygen by bacteria
end
%---------------------------------------------
function u0 = pdex1ic(x) % Initial conditions

u0 = 0; %Oxygen Concentration zero everywhere initially
end
```

```
%---------------------------------------------
function [pl,ql,pr,qr] = pdex1bc(xl,ul,xr,ur,t) % Boundary conditions
pl = ul; % Concentration = zero boundary condition in inner gel (x=0)
ql = 0; % flux coefficient zero in inner gel (x=0)
pr = ur-8; % Concentration = 8 mol/m^3 boundary condition in outer gel (x=xf )ur-8=0
translates to ur=8 mol/m^3
qr = 0; % flux coefficient zero in inner gel (x=xf m)
end
%---------------------------------------------
```

10.4: The iterative for-loop partial differential solver, showing varying diffusion coefficients and porosity.

```
dt=60; XF=0.1; XTOTALDIV =100;
nh=10;
xdivisions=XTOTALDIV/nh;
dx=XF/XTOTALDIV;
p=[0.9,0.8,0.7];
DC=[1.79E-11,1.79E-10,1.79E-09];
for tn=1:2
      for hd=1:3
      if hd==1
   xf1=XF; %Outer hydrogel x value and mesh divisions in spatial coordinate
 x1 = linspace(xf1-10*dx,xf1,xdivisions); %spatial mesh
t1 = linspace(dt*(tn-1),dt*tn,3); % Time points for solution calculation
m = 0;
sol = pdepe(m,@pdex1pde1,@pdex1ic1,@pdex1bc1,x1,t1);
c1 = sol(:,:,1);
elseif hd==2
   xf2=xf-(hd-1)*10*dx; xdivisions=10; %Outer hydrogel x value and mesh divisions in
spatial coordinate
x2 = linspace(xf2-10*dx,xf2,xdivisions); %spatial mesh
t2 = linspace(dt*(tn-1),dt*tn,10); % Time points for solution calculation
m = 0;
sol = pdepe(m,@pdex1pde2,@pdex1ic2,@pdex1bc2,x2,t2);
c2 = sol(:,:,1);
      elseif hd==3
  xf3=xf-(hd-1)*10*dx; xdivisions=10; %Outer hydrogel x value and mesh divisions in
spatial coordinate
x3 = linspace(xf3-10*dx,xf3,xdivisions); %spatial mesh
t3 = linspace(dt*(tn-1),dt*tn,10); % Time points for solution calculation
m = 0;
sol = pdepe(m,@pdex1pde3,@pdex1ic3,@pdex1bc3,x3,t3);
c3 = sol(:,:,1);
end
```

```
    end

end
% xf=10; xdivisions=100; %Outer hydrogel x value and mesh divisions in spatial coordinate
% x = linspace(0,xf,xdivisions); %spatial mesh
% t = linspace(0,400,40); % Time points for solution calculation
% m = 0;
% sol = pdepe(m,@pdex1pde,@pdex1ic,@pdex1bc,x,t);
% u = sol(:,:,1);
% figure
% surf(x,t,u)
% title('Oxygen Concentration (mol/m^3)')
% xlabel('Distance x')
% ylabel('Time t')
% figure
% surf(x,t,exp(-t)'*sin(pi*x))
% title('True solution plotted with 20 mesh points')
% xlabel('Distance x')
% ylabel('Time t')

% figure
% plot(x,u(end,:),'o',x,exp(-t(end))*sin(pi*x))
% title('Solution at t = 2')
% legend('Numerical, 20 mesh points','Analytical','Location','South')
% xlabel('Distance x')
% ylabel('u(x,2)')

function [c,f,s] = pdex1pde1(x,t,u,dudx) % Equation to solve
c = p(1);
f = (dudx)*DC(1); %D=1.79E-8; %diffusion coefficient for 3% alginate (Hulst et.al. 1989)
s = 0;
end
%--------------------------------------------
function u0 = pdex1ic1(x) % Initial conditions

u0 = 0;
end
%--------------------------------------------
function [pl,ql,pr,qr] = pdex1bc1(xl,ul,xr,ur,t) % Boundary conditions
pl = ul;
ql = 0;
pr = ur-0.28;
qr = 0;
end
```

```
function [c,f,s] = pdex1pde2(x,t,u,dudx) % Equation to solve
c = p(2);
f = (dudx)*DC(2); %D=1.79E-8; %diffusion coefficient for 3% alginate (Hulst et.al. 1989)
s = 0;
end
%---------------------------------------------
function u0 = pdex1ic2(x) % Initial conditions

u0 = 0;
end
%---------------------------------------------
function [pl,ql,pr,qr] = pdex1bc2(xl,ul,xr,ur,t) % Boundary conditions
pl = ul;
ql = 0;
pr = ur-c1(1);
qr = 0;
end


function [c,f,s] = pdex1pde3(x,t,u,dudx) % Equation to solve
c = p(3);
f = (dudx)*DC(3); %D=1.79E-8; %diffusion coefficient for 3% alginate (Hulst et.al. 1989)
s = 0;
end
%---------------------------------------------
function u0 = pdex1ic3(x) % Initial conditions

u0 = 0;
end
%---------------------------------------------
function [pl,ql,pr,qr] = pdex1bc3(xl,ul,xr,ur,t) % Boundary conditions
pl = ul;
ql = 0;
pr = ur-c2(1);
qr = 0;
end

%---------------------------------------------
```

10.5 The initial Crank-Nicholson model, showing the initial matrix to be solved

```
%This program is meant to test out the Crank-Nicolson scheme using a simple
%linear 1D diffusion od concentration in a slab  dC/dt = D*d^2(C)/dt^2.
%Initial Condition c=0.28 mol/m^3 at x=L
%Boundary Condition at x=0, c= 0 and at x=L, c=0.28 mol/m^3 a
tn=1000; % no of time steps
tmax=144000; % Tmax in sec, Tmax/3600 = 144000/3600 = 40 hrs
m=100;  % No of x-grid points
L=0.1; % Thicknes of Hydrogel
t=linspace(0,tmax,tn);% set time and distance scales
x=linspace(0,L,m); % distancce
dx=x(2)-x(1); %grid spacing in meters
dt=t(2)-t(1); %Time step in seconds
%s=dt*1.79E-8/(2*dx^2);%Useful for the solution alpha.
C=zeros(tn,m); %set up solution matrix
A=zeros(m,m);  % Coefficent matrix for solving systen of equations AC=d
A(1,1) = 1; % For setting boundary condition at x=0, c=0
A(1,2) = 0; % For setting boundary condition at x=0, c=0
DC=1.79E-8; %Diffusion Coefficient
s=DC*dt/(2*dx^2);%Useful for calculating tridiagonal matrix elements.
% Basis Triadiangonal system (Crank-Nicholson) AC=d, i - next time, j- current spatial
cordinate
% -s*C(i,j-1)+(1+2*s)*C(i,j)-s*C(i,j+1) = s*C(i-1,j+1)+(1-2*s)*C(i-1,j)+s*C(i-1,j-1);
% Build tridiagonal coefficeint matrix A for solving system of equations AC=d
for j=2:m-1
   %s= DCOF(j,1)*dt/(2*dx^2);
     A(j,j-1) = -s; % lower diaginal element
  A(j,j) = (1+2*s); % diagonal element
  A(j,j+1) = -s; % upper diagonal element
end
A(m,m-1)= 0; % For setting boundary condition at x=L
A(m,m) = 1; % For setting boundary condition at x=L
%Add in intial condition:
C(1,:)=0; % t=0, first row in solution matrix C
d=zeros(m,1);
co=0.28; %0.28 Oxygen Concentration mol/m^3 at x=L;
C(:,m)=ones(tn,1).*co; % Boundary Condition at x=L;
%d0=C(1,1:m)'; % Initial Condition c=0 everywhere except at L, c=co
% %generate matrix A
%Solve the system
for i=2:tn
  %Construct the RHS for the solution
  %d=C(1,1:m)'; % Initial Condition c=0 everywhere except at L, c=co
```

```
  d(1)=0; % Boundary condition at x=0, c =0
  d(m)=0.28; % Boundary condition at x=L, c = 0.28 mol/m^3
  for j=2:m-1
     d(j)=s*C(i-1,j+1)+(1-2*s)*C(i-1,j)+s*C(i-1,j-1);
  end
  %Solve for the new time step
  w=A\d; % w is the solution, concentration in current step
  C(i,2:m-1)=w(2:m-1,1); %assing current solution to solution matrix C to ith row
end
% figure
% surf(x,t./3600,C) % Convert time to hrs
% title('Oxygen Concentration (mol/m^3)')
% xlabel('Distance (m)')
% ylabel('Time (h)')

figure
p1=plot(x,C(1,:),'o')
hold
title('Oxygen Concentration (mol/m^3)')
xlabel('Distance (m)')
ylabel('Oxygen Concentration (mol/m^3)')
for i=1:tn/100-1
     plot(x,C(i*100,:))
end
pend = plot(x,C(tn,:),'--')
legend([p1 pend],{'t=0','t=40 hr'})% tmax = tmax/3600 hrs
hold

% nh=10; % no fo hydrogels
% nhm=m/10;
% DCOF=zeros(m,1); % Array for diffusion coefficeints in m^2/s
% %generate array for Diffusion Coefficients for each Hydrogel
% % Fill Diffusion Coefficient for inner and outer hydrogels
%     DCOF(1:nhm,1)=1*1.79E-12; % Diffusion Coefficient for inner Hydrogel
%     DCOF(m-nhm:m,1)=1*1.79E-8; % Diffusion Coefficient for outer Hydrogel
% for i = 1:nh-1
%     %b(i,1)=i;
%       DCOF(i*nhm:(i+1)*nhm,1)=(i+1)*1.79E-8;% Diffusion Coefficient for inner
Hydrogels
% end
```

10.6: Improvements on the initial code through the implementation of an upwind scheme.

```
%**************************************
% Governing equation:
% dC/dt = D * [ 1/r * dC/dr + d^2C/dr^2  ]
% where C is mass concentration, D is diffusion coefficient, t is time, r
%   is radial direction
%
% Boundary conditions:
% At the outer boundary of most outer layer: C = constant_1
% At the inner boundary of most inner layer: C = constant_2
% At interfaces between layers:
%      C_{left} = C_{right}
%      (D*dC/dr)_{left} = D*dC/dr_{right}
%**************************************
%
%**************************************
% Using Crank Nicolson Method
% Define: dt = t^{n+1} - t^{n}
% dC/dt = [C^{n+1}_{i} - C^{n}_{i}]/dt
% Spacial derivatives are represented by the average of current time step
% t^{n} and next time step t^{n+1}
% Define: h is spacial step in finite difference method
% dC/dr = 1/2 * [ (C^{n+1}_{i+1} - C^{n+1}_{i})/h
%              +(C^{n  }_{i+1} - C^{n  }_{i})/h ]
% Note here we only use the first order FDM for dC/dr
% This is a normal numerical trick for diffusion (d/dr)
%   to keep the numerical method stable
% For more information, please refer to upwind scheme:
%   https://en.wikipedia.org/wiki/Upwind_scheme
% Since we know the mass will diffuse from node m to node 1, we choose to
%   ues information from i+1 to calculate dC/dr
% d^2C/dr^2 = 1/2 * [ (C^{n+1}_{i+1} - 2C^{n+1}_{i} + C^{n+1}_{i-1})/h^2
%                  +(C^{n  }_{i+1} - 2C^{n  }_{i} + C^{n  }_{i-1})/h^2 ]
%
% Boundary conditions:
%   C(1) = constant_1
%   C(m) = constant_2
% At interface with node j:
%   D_{left} * 1/2 * [ (C^{n+1}_{i} - C^{n+1}_{i-1})/h
%                   +(C^{n  }_{i} - C^{n  }_{i-1})/h]
% = D_{right}* 1/2 * [ (C^{n+1}_{i+1} - C^{n+1}_{i})/h
%                   +(C^{n  }_{i+1} + C^{n  }_{i})/h]
```

```
% Once again, the upwind scheme is used
%**************************************
%

clear;

tn = 5000;     % no of time steps
tmax = 216000;  % max simulation time
t = linspace(0,tmax,tn);    % set time and distance scales
dt = t(2)-t(1);     % Time Increment - dt

m = 201;    % No of r-grid point
rmin = 0.0; % most inner boundary r
rmax = 0.1; % most outer boundary r
r = linspace(rmin,rmax,m);  % distancce
dr = r(2)-r(1);     % Spacial increment - h

nh = 10; % no of hydrogels
nhm = (m-1)/nh;

DCOF = zeros(m,1); % Array for diffusion coefficeints in m^2/s
% Diffusion Coefficient for Hydrogel at each layer
for i = 0 : nh-1
   DCOF(i*nhm+1: (i+1)*nhm, 1) = (i*1+1) * 1.79E-9;
end
DCOF(1,1) = 0;
DCOF(m,1) = 0;

interfaceID = zeros(nh-1,1); % node id to record interface location
interfaceID(1,1) = 10;    % node id of interface 1-2
interfaceID(2,1) = 20;    % node id of interface 2-3
interfaceID(3,1) = 30;    % node id of interface 3-4
interfaceID(4,1) = 40;    % node id of interface 4-5
interfaceID(5,1) = 50;    % node id of interface 5-6
interfaceID(6,1) = 60;    % node id of interface 6-7
interfaceID(7,1) = 70;    % node id of interface 7-8
interfaceID(8,1) = 80;    % node id of interface 8-9
interfaceID(9,1) = 90;    % node id of interface 9-10


C = zeros(tn,m); % Concentration to be solved

A = zeros(m,m);  % Coefficent matrix for solving systen of equations AC=d
```

```
A(1,1) = 1; % At the inner boundary of most inner layer: C = constant_2
A(m,m) = 1; % At the outer boundary of most outer layer: C = constant_1

%Set up matrix A to solve C^{n+1}
for i = 2 : m-1

   iflag = 0;

   % At interfaces
   for j = 1 : nh-1
      if i == interfaceID(j,1)

         sl = DCOF(i-1,1)/(2*dr);
         sr = DCOF(i+1,1)/(2*dr);
         A(i,i  ) = sr + sl;
         A(i,i-1) =-sl;
         A(i,i+1) =-sr;

         iflag = 1;

      end
   end

   if iflag == 1   % We have set up the BC at the interface
      continue
   end

   s = DCOF(i,1)*dt/(2*dr^2);
   A(i,i-1) = s;
   A(i,i+1) = s+s*dr/r(i);
   A(i,i  ) =-s*2-s*dr/r(i) - 1;

end

C(1,:) = 0; % Intial condition at t = 0

% Boundary conditions
ci = 0;    %    0 Oxygen Concentration mol/m^3 at r=rmin;
co = 0.28; % 0.28 Oxygen Concentration mol/m^3 at r=rmax;

%Solve the system
for n = 1 : tn-1

   d = zeros(m,1);
```

```
% Construct the RHS for the solution
d(1) = ci;
d(m) = co;

for i = 2 : m-1

   iflag = 0;

   % At interfaces
   for j = 1 : nh-1
      if i == interfaceID(j,1)

         sl = DCOF(i-1,1)/(2*dr);
         sr = DCOF(i+1,1)/(2*dr);
         d(i) = sr*C(n,i+1) + sl*C(n,i-1) - (sr+sl)*C(n,i);

         iflag = 1;

      end
   end

   if iflag == 1   % We have set up the BC at the interface
      continue
   end

   s = DCOF(i,1)*dt/(2*dr^2);

%       d(i) =-s*C(n,i-1)-(s+s*dr/r(i))*C(n,i+1)+(s*2+s*dr/r(i)-1)*C(n,i);

   if i > 40 && i < 50

      oa=148.5;
      ob=0.2805;

      if n == 1
         oc1 = 0;
      else
         [oc1] = oxcoms(t(n-1),oa,ob);
      end
      [oc2] = oxcoms(t(n),oa,ob);

      source = dt/2 * (oc1 + oc2);
```

```
            d(i) =-s*C(n,i-1)-(s+s*dr/r(i))*C(n,i+1)+(s*2+s*dr/r(i)-1)*C(n,i)...
                +source;

        else

            d(i) =-s*C(n,i-1)-(s+s*dr/r(i))*C(n,i+1)+(s*2+s*dr/r(i)-1)*C(n,i);

        end

    end

    % Solve for the new time step
    w = A\d;
    C(n+1,2:m-1) = w(2:m-1,1); % update concentration to the next step
    C(n+1,1) = ci;  %    0 Oxygen Concentration mol/m^3 at r=rmin;
    C(n+1,m) = co;  % 0.28 Oxygen Concentration mol/m^3 at r=rmax;

end

% figure
% surf(r,t./3600,C) % Convert time to hrs
% title('Oxygen Concentration (mol/m^3)')
% xlabel('Radius(m)')
% ylabel('Time (h)')

figure
p1 = plot(r,C(1,:),'o');
hold
title('Axisymm Variable Diffusion Coefficient for each Hydrogel')
xlabel('Radius (m)')
ylabel('Oxygen Concentration (mol/m^3)')
for i = 1 : tn/500-1
    plot(r,C(i*500,:))
end
pend = plot(r,C(tn,:),'--');
legend([p1 pend],{'t=0','t=tmax'})  % tmax = tmax/3600 hrs
hold
Tmaxinhrs = tmax/3600;



function [oc1] = oxcoms(t1,oa,ob) % Equation to solve

    ox=5./(oa*exp(-ob*t1)+1); %cells in g
```

```
    oc1=ox*10E-12*0.74; %true value, may be modified to show effects

end
```

10.7: The final CN code, showing places for 10 hydrogels and 10 oxygen coefficients

```
%****************************************
% Governing equation:
% dC/dt = D * [ 1/r * dC/dr + d^2C/dr^2  ]
% where C is mass concentration, D is diffusion coefficient, t is time, r
%   is radial direction
%
% Boundary conditions:
% At the outer boundary of most outer layer: C = constant_1
% At the inner boundary of most inner layer: C = constant_2
% At interfaces between layers:
%      C_{left} = C_{right}
%      (D*dC/dr)_{left} = D*dC/dr_{right}
%****************************************
%
%****************************************
% Using Crank Nicolson Method
% Define: dt = t^{n+1} - t^{n}
% dC/dt = [C^{n+1}_{i} - C^{n}_{i}]/dt
% Spacial derivatives are represented by the average of current time step
% t^{n} and next time step t^{n+1}
% Define: h is spacial step in finite difference method
% dC/dr = 1/2 * [ (C^{n+1}_{i+1} - C^{n+1}_{i})/h
%               +(C^{n  }_{i+1} - C^{n  }_{i})/h ]
% Note here we only use the first order FDM for dC/dr
% This is a normal numerical trick for diffusion (d/dr)
%   to keep the numerical method stable
% For more information, please refer to upwind scheme:
%   https://en.wikipedia.org/wiki/Upwind_scheme
% Since we know the mass will diffuse from node m to node 1, we choose to
%   ues information from i+1 to calculate dC/dr
% d^2C/dr^2 = 1/2 * [ (C^{n+1}_{i+1} - 2C^{n+1}_{i} + C^{n+1}_{i-1})/h^2
%                   +(C^{n  }_{i+1} - 2C^{n  }_{i} + C^{n  }_{i-1})/h^2 ]
%
% Boundary conditions:
%   C(1) = constant_1
```

```
%   C(m) = constant_2
% At interface with node j:
%   D_{left} * 1/2 * [ (C^{n+1}_{i} - C^{n+1}_{i-1})/h
%                     +(C^{n  }_{i} - C^{n  }_{i-1})/h]
% = D_{right}* 1/2 * [ (C^{n+1}_{i+1} - C^{n+1}_{i})/h
%                     +(C^{n  }_{i+1} + C^{n  }_{i})/h]
% Once again, the upwind scheme is used
%**************************************
%
% This code follows the style of Srinivas' code
%
%
%

clear;

tn = 5000;     % no of time steps
tmax = 216000;  % max simulation time
t = linspace(0,tmax,tn);    % set time and distance scales
dt = t(2)-t(1);     % Time Increment - dt

m = 201;    % No of r-grid point
rmin = 0.0; % most inner boundary r
rmax = 0.1; % most outer boundary r
r = linspace(rmin,rmax,m);  % distancce
dr = r(2)-r(1);     % Spacial increment - h

nh = 10; % no of hydrogels
nhm = (m-1)/nh;

DCOF = zeros(m,1); % Array for diffusion coefficeints in m^2/s
% Diffusion Coefficient for Hydrogel at each layer
for i = 0 : nh-1
   DCOF(i*nhm+1: (i+1)*nhm, 1) = (i*1+1) * 1.79E-9;
end
DCOF(1,1) = 0;
DCOF(m,1) = 0;

interfaceID = zeros(nh-1,1); % node id to record interface location
interfaceID(1,1) = 10;    % node id of interface 1-2
interfaceID(2,1) = 20;    % node id of interface 2-3
interfaceID(3,1) = 30;    % node id of interface 3-4
interfaceID(4,1) = 40;    % node id of interface 4-5
interfaceID(5,1) = 50;    % node id of interface 5-6
```

```
interfaceID(6,1) = 60;    % node id of interface 6-7
interfaceID(7,1) = 70;    % node id of interface 7-8
interfaceID(8,1) = 80;    % node id of interface 8-9
interfaceID(9,1) = 90;    % node id of interface 9-10


C = zeros(tn,m); % Concentration to be solved

A = zeros(m,m);  % Coefficent matrix for solving systen of equations AC=d

A(1,1) = 1; % At the inner boundary of most inner layer: C = constant_2
A(m,m) = 1; % At the outer boundary of most outer layer: C = constant_1

%Set up matrix A to solve C^{n+1}
for i = 2 : m-1

   iflag = 0;

   % At interfaces
   for j = 1 : nh-1
      if i == interfaceID(j,1)

         sl = DCOF(i-1,1)/(2*dr);
         sr = DCOF(i+1,1)/(2*dr);
         A(i,i  ) = sr + sl;
         A(i,i-1) =-sl;
         A(i,i+1) =-sr;

         iflag = 1;

      end
   end

   if iflag == 1   % We have set up the BC at the interface
      continue
   end

   s = DCOF(i,1)*dt/(2*dr^2);
   A(i,i-1) = s;
   A(i,i+1) = s+s*dr/r(i);
   A(i,i) =-s*2-s*dr/r(i) - 1;

end
```

```
C(1,:) = 0; % Intial condition at t = 0

% Boundary conditions
ci = 0;    %    0 Oxygen Concentration mol/m^3 at r=rmin;
co = 0.28; % 0.28 Oxygen Concentration mol/m^3 at r=rmax;

%Solve the system
for n = 1 : tn-1

   d = zeros(m,1);

   % Construct the RHS for the solution
   d(1) = ci;
   d(m) = co;

   for i = 2 : m-1

      iflag = 0;

      % At interfaces
      for j = 1 : nh-1
         if i == interfaceID(j,1)

            sl = DCOF(i-1,1)/(2*dr);
            sr = DCOF(i+1,1)/(2*dr);
            d(i) = sr*C(n,i+1) + sl*C(n,i-1) - (sr+sl)*C(n,i);

            iflag = 1;

         end
      end

      if iflag == 1   % We have set up the BC at the interface
         continue
      end

      s = DCOF(i,1)*dt/(2*dr^2);

%       d(i) =-s*C(n,i-1)-(s+s*dr/r(i))*C(n,i+1)+(s*2+s*dr/r(i)-1)*C(n,i);

      if i > 1 && i < nhm % calling first function for first inner hydrogel

         oa=148.5;
         ob=0.2805;
```

```
    if n == 1
       oc1 = 0;
    else
       [oc1] = oxcoms(t(n-1),oa,ob);
    end
    [oc2] = oxcoms(t(n),oa,ob);

    source1 = dt/2 * (oc1 + oc2);

    d(i) =-s*C(n,i-1)-(s+s*dr/r(i))*C(n,i+1)+(s*2+s*dr/r(i)-1)*C(n,i)...
         +source1;

  else

     %d(i) =-s*C(n,i-1)-(s+s*dr/r(i))*C(n,i+1)+(s*2+s*dr/r(i)-1)*C(n,i);
     if i > nhm && i < 2*nhm %calling second function for second inner hydrogel

    oa=148.5;
    ob=0.2805;

    if n == 1
       oc3 = 0;
    else
       [oc3] = oxcoms2(t(n-1),oa,ob);
    end
    [oc4] = oxcoms2(t(n),oa,ob);

    source2 = dt/2 * (oc3 + oc4);

    d(i) =-s*C(n,i-1)-(s+s*dr/r(i))*C(n,i+1)+(s*2+s*dr/r(i)-1)*C(n,i)...
         +source2;
 else

     %d(i) =-s*C(n,i-1)-(s+s*dr/r(i))*C(n,i+1)+(s*2+s*dr/r(i)-1)*C(n,i);
     if i > 2*nhm && i < 3*nhm %calling third function for second inner hydrogel

    oa=148.5;
    ob=0.2805;

    if n == 1
       oc5 = 0;
    else
       [oc5] = oxcoms3(t(n-1),oa,ob);
```

```
        end
        [oc6] = oxcoms3(t(n),oa,ob);

        source2 = dt/2 * (oc5 + oc6);

        d(i) =-s*C(n,i-1)-(s+s*dr/r(i))*C(n,i+1)+(s*2+s*dr/r(i)-1)*C(n,i)...
            +source2;
    else

        %d(i) =-s*C(n,i-1)-(s+s*dr/r(i))*C(n,i+1)+(s*2+s*dr/r(i)-1)*C(n,i);
        if i > 3*nhm && i < 4*nhm %calling fourth function for second inner hydrogel

        oa=148.5;
        ob=0.2805;

        if n == 1
           oc7 = 0;
        else
           [oc7] = oxcoms4(t(n-1),oa,ob);
        end
        [oc8] = oxcoms4(t(n),oa,ob);

        source2 = dt/2 * (oc7 + oc8);

        d(i) =-s*C(n,i-1)-(s+s*dr/r(i))*C(n,i+1)+(s*2+s*dr/r(i)-1)*C(n,i)...
            +source2;
    else

        %d(i) =-s*C(n,i-1)-(s+s*dr/r(i))*C(n,i+1)+(s*2+s*dr/r(i)-1)*C(n,i);
        if i > 4*nhm && i < 5*nhm %calling fifth function for second inner hydrogel

        oa=148.5;
        ob=0.2805;

        if n == 1
           oc9 = 0;
        else
           [oc9] = oxcoms5(t(n-1),oa,ob);
        end
        [oc10] = oxcoms5(t(n),oa,ob);

        source2 = dt/2 * (oc9 + oc10);

        d(i) =-s*C(n,i-1)-(s+s*dr/r(i))*C(n,i+1)+(s*2+s*dr/r(i)-1)*C(n,i)...
```

```
        +source2;
else

    %d(i) =-s*C(n,i-1)-(s+s*dr/r(i))*C(n,i+1)+(s*2+s*dr/r(i)-1)*C(n,i);
    if i > 6*nhm && i < 7*nhm %calling seventh function for second inner hydrogel

    oa=148.5;
    ob=0.2805;

    if n == 1
       oc11 = 0;
    else
       [oc11] = oxcoms7(t(n-1),oa,ob);
    end
    [oc12] = oxcoms7(t(n),oa,ob);

    source2 = dt/2 * (oc11 + oc12);

    d(i) =-s*C(n,i-1)-(s+s*dr/r(i))*C(n,i+1)+(s*2+s*dr/r(i)-1)*C(n,i)...
        +source2;
else

    %d(i) =-s*C(n,i-1)-(s+s*dr/r(i))*C(n,i+1)+(s*2+s*dr/r(i)-1)*C(n,i);
    if i > 7*nhm && i < 8*nhm %calling eighth function for second inner hydrogel

    oa=148.5;
    ob=0.2805;

    if n == 1
       oc13 = 0;
    else
       [oc13] = oxcoms8(t(n-1),oa,ob);
    end
    [oc14] = oxcoms8(t(n),oa,ob);

    source2 = dt/2 * (oc13 + oc14);

    d(i) =-s*C(n,i-1)-(s+s*dr/r(i))*C(n,i+1)+(s*2+s*dr/r(i)-1)*C(n,i)...
        +source2;

else

    %d(i) =-s*C(n,i-1)-(s+s*dr/r(i))*C(n,i+1)+(s*2+s*dr/r(i)-1)*C(n,i);
    if i > 8*nhm && i < 9*nhm %calling ninth function for second inner hydrogel
```

```
        oa=148.5;
        ob=0.2805;

        if n == 1
           oc15 = 0;
        else
           [oc15] = oxcoms8(t(n-1),oa,ob);
        end
        [oc15] = oxcoms8(t(n),oa,ob);

        source2 = dt/2 * (oc14 + oc15);

        d(i) =-s*C(n,i-1)-(s+s*dr/r(i))*C(n,i+1)+(s*2+s*dr/r(i)-1)*C(n,i)...
             +source2;
    else

        %d(i) =-s*C(n,i-1)-(s+s*dr/r(i))*C(n,i+1)+(s*2+s*dr/r(i)-1)*C(n,i);
        if i > 9*nhm && i < 10*nhm %calling tenth function for second inner hydrogel

        oa=148.5;
        ob=0.2805;

        if n == 1
           oc17 = 0;
        else
           [oc17] = oxcoms8(t(n-1),oa,ob);
        end
        [oc16] = oxcoms8(t(n),oa,ob);

        source2 = dt/2 * (oc16 + oc17);

        d(i) =-s*C(n,i-1)-(s+s*dr/r(i))*C(n,i+1)+(s*2+s*dr/r(i)-1)*C(n,i)...
             +source2;
        else
             d(i) =-s*C(n,i-1)-(s+s*dr/r(i))*C(n,i+1)+(s*2+s*dr/r(i)-1)*C(n,i);

        end
        end
        end
        end
        end
        end
        end
```

```
        end
        end
        end

    % Solve for the new time step
    w = A\d;
    C(n+1,2:m-1) = w(2:m-1,1); % update concentration to the next step
    C(n+1,1) = ci;  %    0 Oxygen Concentration mol/m^3 at r=rmin;
    C(n+1,m) = co;  % 0.28 Oxygen Concentration mol/m^3 at r=rmax;

end

% figure
% surf(r,t./3600,C) % Convert time to hrs
% title('Oxygen Concentration (mol/m^3)')
% xlabel('Radius(m)')
% ylabel('Time (h)')

figure
p1 = plot(r,C(1,:),'o');
%p1 = semilogx(r,C(1,:),'o');
hold
title('Axisymm Variable Diffusion Coefficient for each Hydrogel')
xlabel('Radius (m)')
ylabel('Oxygen Concentration (mol/m^3)')
for i = 1 : tn/500-1
     plot(r,C(i*500,:))
      %semilogx(r,C(i*500,:))
end
pend = plot(r,C(tn,:),'--');
%pend = semilogx(r,C(tn,:),'--');
legend([p1 pend],{'t=0','t=tmax'})  % tmax = tmax/3600 hrs
hold
Tmaxinhrs = tmax/3600;



function [oc1] = oxcoms(t1,oa,ob) % Equation to solve

    ox=5./(oa*exp(-ob*t1)+1); %cells in g

    oc1=ox*10E-12*0.74;

end
```

```
function [oc3] = oxcoms2(t1,oa,ob) % Equation to solve

    ox=2/(oa*exp(-ob*t1)+1); %cells in g

    oc3=ox*10E-12*0.74;

 end
function [oc5] = oxcoms3(t1,oa,ob) % Equation to solve

    ox=2/(oa*exp(-ob*t1)+1); %cells in g

    oc5=ox*10E-12*0.74;

end
function [oc7] = oxcoms4(t1,oa,ob) % Equation to solve

    ox=2/(oa*exp(-ob*t1)+1); %cells in g

    oc7=ox*10E-12*0.74;

 end
function [oc9] = oxcoms5(t1,oa,ob) % Equation to solve

    ox=2/(oa*exp(-ob*t1)+1); %cells in g

    oc9=ox*10E-12*0.74;

 end
function [oc11] = oxcoms6(t1,oa,ob) % Equation to solve

    ox=2/(oa*exp(-ob*t1)+1); %cells in g

    oc11=ox*10E-12*0.74;

 end
 function [oc13] = oxcoms7(t1,oa,ob) % Equation to solve

    ox=2/(oa*exp(-ob*t1)+1); %cells in g

    oc13=ox*10E-12*0.74;

 end
 function [oc15] = oxcoms8(t1,oa,ob) % Equation to solve
```

```
    ox=2/(oa*exp(-ob*t1)+1); %cells in g

    oc15=ox*10E-12*0.74;

end
function [oc17] = oxcoms9(t1,oa,ob) % Equation to solve

    ox=2/(oa*exp(-ob*t1)+1); %cells in g

    oc17=ox*10E-12*0.74;

end
function [oc19] = oxcoms10(t1,oa,ob) % Equation to solve

    ox=2/(oa*exp(-ob*t1)+1); %cells in g

    oc19=ox*10E-12*0.74;

end
```

11. Bibliography

Abbasi, B., Mirlohi, M., Daniali, M. & Ghiasvand, R., 2018. Effects of probiotic soymilk on lipid panel in type 2 diabetic patients with nephropathy: A double-blind randomized clinical trial.. *Progress in Nutrition,* pp. 70-78.

AFCAPS/TexCAPS Research Group, 1998. Primary prevention of acute coronary events with lovastatin in men and women with average cholesterol levels: results of AFCAPS/TexCAPS. *Jama,* pp. 1615-1622.

Agarwal, V. et al., 2010. Statin use and the prevention of venous thromboembolism: A meta-analysis.. *International Journal of Clinical Practice,* pp. 1375-1383.

Arjmandi, M. & Ramezani, M., 2019. Finite element modelling of sliding wear in three-dimensional textile hydrogel composites. *Tribology International,* 133(5), pp. 88-100.

Asemi, Z. et al., 2013. Effect of multispecies probiotic supplements on metabolic profiles, hs-CRP, and oxidative stress in patients with type 2 diabetes.. *Annals of nutrition and metabolism,* pp. 1-9.

Australian Institure of Health and Welfare, 2020. *Cardiovascular disease.* [Online] Available at: https://www.aihw.gov.au/reports/heart-stroke-vascular-diseases/cardiovascular-health-compendium/contents/what-is-cardiovascular-disease

Baigent, C. et al., 2009. fficacy and safety of more intensive lowering of LDL cholesterol: a meta-analysis of data from, 170.. *CT Trialists,* pp. 1670-1681.

Ballantyne, C. et al., 2008. Effect of rosuvastatin therapy on coronary artery stenoses assessed by quantitative coronary angiography: a study to evaluate the effect of rosuvastatin on intravascular ultrasound-derived coronary atheroma burden. *Circulation,* pp. 2458-2466.

Bárcena, C., Mayoral, P. & Quirós, P., 2018. Mitohormesis, an Antiaging Paradigm. *International Review on Cellular Molecular Biology,* pp. 340-355.

Bellosta, S. et al., 2004. Statins effect on smooth muscle cell proliferation. *Seminars in Vascular Medicine,* p. 347-356.

Cannon, C. et al., 2004. Pravastatin or Atorvastatin Evaluation and Infection Therapy-Thrombolysis in Myocardial Infarction 22 Investigators. Intensive versus moderate lipid lowering with statins after acute coronary syndromes. *New England Journal of Medicine,* pp. 1495-1504.

Caparrós-Martín, J. et al., 2017. Statin therapy causes gut dysbiosis in mice through a PXR-dependent mechanism. *Microbiome,* pp. 1-15.

Chalasani, N., 2005. Statins and hepatotoxicity: focus on patients with fatty liver. *Hepatology,* pp. 690-695.

Chen, J. et al., 2018. Nitric oxide bioavailability dysfunction involves in atherosclerosis. *Biomedicine & Pharmacotherapy,* pp. 423-428.

Collins, R., 2003. Heart Protection Study Collaborative Group. MRC/BHF Heart Protection Study of cholesterol-lowering with simvastatin in 5963 people with diabetes: a randomised placebo-controlled trial. *Lancet,* pp. 2005-2016.

Cooperative Institute for Meterological Satellite Studies, 2000. *What is matlab?.* [Online] Available at: https://cimss.ssec.wisc.edu/wxwise/class/aos340/spr00/whatismatlab.htm [Accessed 15 10 2020].

Crouse III, J., 2008. An evaluation of rosuvastatin: pharmacokinetics, clinical efficacy and tolerability. *Expert Opinion on Drug Metabolism & Toxicology,* pp. 287-304.

Davis, C., 2014. Enumeration of probiotic strains: Review of culture-dependent and alternative techniques to quantify viable bacteria. *Journal of Microbiological Methods,* 103(August), pp. 9-17.

Di Napoli, A. et al., 2005. Chronic treatment with rosuvastatin modulates nitric oxide synthase expression and reduces ischemia-reperfusion injury in rat hearts.. *Cardiovasc Research,* pp. 462-471.

Ebrahimi, R. et al., 2008. Effect of preprocedural statin use on procedural myocardial infarction and major cardiac adverse events in percutaneous coronary intervention: a meta-analysis. *Journal of Invasive Cardiology,* pp. 292-295.

Egert, M. et al., 2006. Beyond diversity: functional microbiomics of the human colon.. *Trends in microbiology,* pp. 86-91.

Eid, H. et al., 2017. Significance of microbiota in obesity and metabolic diseases and the modulatory potential by medicinal plant and food ingredients. *Frontiers in Pharmacology,* p. 387.

Endrenyi, L., Fritsch, S. & Yan, W., 1991. Cmax/AUC is a clearer measure than Cmax for absorption rates in investigations of bioequivalence.. *International Journal of Clinical Pharmacology and Therapeutics,* pp. 394-399.

Everett, B., Glynn, R., MacFadyen, J. & Ridker, P., 2010. Rosuvastatin in the prevention of stroke among men and women with elevated levels of C-reactive protein. *Circulation,* pp. 143-150.

Fedson, D., 2006. andemic influenza: A potential role for statins in treatment and prophylaxis.. *Clinical Infectious Diseases,* p. 199-205.

Feingold, K. & Grunfeld, C., 2018. Introduction to lipids and lipoproteins. *Endotext,* 1(1), pp. 20-35.

Fellström, B. et al., 2007. Effect of rosuvastatin on outcomes in chronic haemodialysis patients: baseline data from the AURORA study.. *Kidney and Blood Pressure Research,* pp. 314-322.

Fitzpatrick, R., 2006. *Upwind differencing.* [Online]
Available at: http://farside.ph.utexas.edu/teaching/329/lectures/node93.html
[Accessed 15 10 20].

Gaw, A., Packard, C. & Shepherd, J., 1999. *Statins: the HMG CoA reductase inhibitors in perspective..* Chicago: CRC Press.

Giroux, L., Davignon, J. & Naruszewicz, M., 1993. Simvastatin inhibits the oxidation of low-density lipoproteins by activated human monocyte-derived macrophages. *Biochimica et Biophysica Acta,* pp. 335-338.

Glynn, R. et al., 2009. A randomized trial of rosuvastatin in the prevention of venous thromboembolism. *The New England Journal of Medicine,* pp. 1851-1861.

Graham, D. et al., 2004. Incidence of hospitalized rhabdomyolysis in patients treated with lipid-lowering drugs.. *Jama,* pp. 2585-2590.

Grand Challenges, 2020. *About Grand Challenges.* [Online]
Available at: https://gcgh.grandchallenges.org/about
[Accessed 27 March 2020].

Hao, P. et al., 2011. Complete sequencing and pan-genomic analysis of Lactobacillus delbrueckii subsp. bulgaricus reveal its genetic basis for industrial yogurt production.. *PloS one.*

Heart Protection Study Collaborative Group., 2002. Heart Protection Study of antioxidant vitamin supplementation in 20 536 high-risk individuals: a randomised placebo-controlled trial. *Lancet,* pp. 23-33.

Heart Protection Study Collaborative Group, 2002. Heart Protection Study of cholesterol lowering with simvastatin in 20 536 high-risk individuals: a randomised placebocontrolled trial. *The Lancet,* pp. 7-22.

He, X. et al., 2017. Gut microbiota modulation attenuated the hypolipidemic effect of simvastatin in high-fat/cholesterol-diet fed mice. *Journal of proteome research,* pp. 1900-1910.

Hruby, V. & Vardanyan, R., 2016. Hypolipidemic and Antihyperlipidemic Drugs. *Synthesis of Best-Seller Drugs,* 10(1), pp. 285-315.

Hulst, A., Hens, H., Buitelaar, R. & Tramper, J., 1989. Determination of the effective diffusion coefficient of oxygen in gel materials in relation to gel concentration. *Biotechnology Techniques,* 3(3), pp. 199-204.

Ikeda, L., Young, A. & J., L., 2003. Rosuvastatin, a new HMG-CoA reductase inhibitor, protects ischemic reperfused myocardium in normocholesterolemic rats. *Journal of Cardiovascular Pharmacology,* pp. 649-656.

Inoue, I. et al., 2000. Lipophilic HMG-CoA reductase inhibitor has an anti-inflammatory effect: Reduction of mRNA levels for interleukin-1beta, interleukin-6, cyclooxygenase-2, and p22phox by regulation of peroxisome proliferator-activated receptor alpha (PPARalpha) in primary e. *Life Science,* pp. 863-876.

Johnson, F. H., 1936. The Oxygen Uptake of Marine Bacteria. *Journal of Bacteriology,* 31(5), pp. 547-556.

Jones, M., Martoni, C., Parent, M. & Prakash, S., 2012. Cholesterol-lowering efficacy of a microencapsulated bile salt hydrolase-active Lactobacillus reuteri NCIMB 30242 yoghurt formulation in hypercholesterolaemic adults. *British Journal of Nutrition,* pp. 1505-1513.

Kamio, K. et al., 2010. Statins inhibit matrix metalloproteinase release from human lung fibroblasts. *European Respiratory Journal,* pp. 247-256.

Khan, M. H. M. et al., 2020. Global Epidemiology of Ischemic Heart Disease Results from the Global Burden of Disease Study. *Cureus.*

Khan, T. Y. et al., 2018. Effect of atorvastatin on the gut microbiota of high fat diet-induced hypercholesterolemic rats. *Scientific reports,* p. 662.

Kodaman, P. & Duleba, A., 2008. Statins in the treatment of polycystic ovary syndrome. *Seminars in Reproductive Medicine,* pp. 127-138.

Kolbeck, S., Reetz, L., Hilgarth, M. & Vogel, R. F., 2019. Quantitative Oxygen Consumption and Respiratory Activity of Meat Spoiling Bacteria Upon High Oxygen Modified Atmosphere. *Frontiers in Microbiology,* 10(November), p. 2398.

Liao, J. & Laufs, U., 2005. Pleiotropic effects of statins. *Annual Review Pharmacology Toxicology,* pp. 89-118.

Liu, Y. et al., 2018. Gut microbiome associates with lipid-lowering effect of rosuvastatin in vivo. *Front Microbiology,* pp. 530-539.

Lloyd, S. et al., 2013. Long-term effects of statin treatment in elderly people: extended follow-up of the PROspective Study of Pravastatin in the Elderly at Risk (PROSPER Study). *PLoS One,* p. 8.

Long-Term Intervention with Pravastatin in Ischaemic Disease (LIPID) Study Group, 1998. revention of cardiovascular events and death with pravastatin in patients with coronary heart disease and a broad range of initial cholesterol levels.. *New England Journal of Medicine,* pp. 1349-1357.

Madjd, A. et al., 2016. Comparison of the effect of daily consumption of probiotic compared with low-fat conventional yogurt on weight loss in healthy obese women following an energy-restricted diet: a randomized controlled trial.. *The American journal of clinical nutrition,* pp. 323-329.

Maron, D., Fazio, S. & Linton, M., 2000. Current perspectives on statins. *Circulation,* p. 207–213.

Martin, D. S., 1932. The Oxygen Consumption of Escherichia Coli During the Lag and Logarithmic Phases of Growth. *The Journal of General Physiology,* pp. 691-709.

Martínez-González, J., Raposo, B. & Rodriguez, C., 2001. 3-Hydroxy-3-methylglutaryl coenzyme A reductase inhibition prevents endothelial NO synthase downregulation by atherogenic levels of native LDLs: balance between transcriptional and posttranscriptional regulation. *Arteriosclerosis, Thrombosis, and Vascular Biology,* p. 804–809.

Mathur, N., Ramasubbu, K. & Mann, D., 2008. Spectrum of pleiotropic effects of statins in heart failure. *Heart Failure Clinics,* pp. 153-161.

MATLAB, 2020. *pdepe.* [Online]
Available at: https://au.mathworks.com/help/matlab/ref/pdepe.html
[Accessed 15 10 2020].

McDonnell, A. & Dang, C., 2013. Basic review of the cytochrome p450 system. *Journal of the advanced practitioner in oncology,* p. 263.

McTaggart, F. et al., 2001. American Journal of Cardiology. *Preclinical and clinical pharmacology of Rosuvastatin, a new 3-hydroxy-3-methylglutaryl coenzyme A reductase inhibitor.,* pp. 28-32.

McTavish, D. & Sorkin, E., 1991. Pravastatin. A review of its pharmacological properties and therapeutic potential in hypercholesterolaemia. *Drugs ,* pp. 65-89.

Meganathan, R. & Kwon, O., 2009. Biosynthesis of Menaquinone (Vitamin K2) and Ubiquinone (Coenzyme Q). *EcoSal Plus,* 3(Sept).

Miranda, P. et al., 2018. High salt diet exacerbates colitis in mice by decreasing Lactobacillus levels and butyrate production. *Microbiome,* pp. 1-17.

Mizushima, S. et al., 2004. Randomized controlled trial of sour milk on blood pressure in borderline hypertensive men.. *American journal of hypertension,* pp. 701-706.

Musso, G., Gambino, R. & Cassader, M., 2011. Interactions between gut microbiota and host metabolism predisposing to obesity and diabetes. *Annual Review in Medicine,* pp. 361-380.

Neto-Ferreira, V., Novaes Rocha, T., da Silva Torres, C. & Mandarim-de-Lacerda, J. d. C., 2011. Beneficial effects of rosuvastatin on aortic adverse remodeling in nitric oxide-deficient rats. *Expert Toxicology Pathology,* pp. 473-478.

Nichols, M., Townsend, N., Scarborough, P. & Rayner, M., 2014. Cardiovascular disease in Europe 2014: epidemiological update. *European Heart Journal,* pp. 2950-2959.

Nissen, S. et al., 2004. Effect of intensive compared with moderate lipid-lowering therapy on progression of coronary atherosclerosis: a randomized controlled trial. *Jama,* pp. 1071-1080.

Nolan, J. et al., 2017. The influence of rosuvastatin on the gastrointestinal microbiota and host gene expression profiles. *American Journal of Physiology-Gastrointestinal and Liver Physiology,* pp. 488-497.

Olsson, A., McTaggart & Raza, A., 2002. Rosuvastatin: a highly effective new HMG-CoA reductase inhibitor. *Cardiovascular Drug Review,* pp. 303-328.

Our World Data, 2016. *Burden of Disease.* [Online]
Available at: https://ourworldindata.org/burden-of-disease.

Pimenta, A., Serro, A. P., Colaço, R. & Chauhan, A., 2019. Optimization of intraocular lens hydrogels for dual drug release: Experimentation and modelling. *European Journal of Pharmaceutics and Biopharmaceutics,* 141(August), pp. 51-57.

PubChem, 2020. *(3R,5S,6E)-7-[4-(4-Fluorophenyl)-2-[(methanesulfonyl)(methyl)amino]-6-(propan-2-yl)pyrimidin-5-yl]-3,5-dihydroxyhept-6-enoic acid.* [Online]
Available at: https://pubchem-ncbi-nlm-nih-gov.ezproxy.lib.rmit.edu.au/substance/387075810

Ray, K. et al., 2005. Early and late benefits of high-dose atorvastatin in patients with acute coronary syndromes: results from the PROVE IT-TIMI 22 trial. *Journal of the American College of Cardiology,* pp. 1405-1410.

Rezaei, M. et al., 2017. The effect of probiotic yogurt on blood glucose and cardiovascular biomarkers in patients with type II diabetes: a randomized controlled trial. *Evidence Based Care,* pp. 26-35.

Rezvani, F., Ardestani, F. & Najafpour, G., 2017. Growth kinetic models of five species of Lactobacilli and lactose consumption in batch submerged culture. *Brazilian Journal of Microbiology,* 48(2), pp. 251-258.

Ridker, P. et al., 2008. Rosuvastatin to prevent vascular events in men and women with elevated C-reactive protein.. *New England journal of medicine,* pp. 2195-2207.

Rowland, K. & Malcolm, H., 1972. Influence of route of administration on drug availability. *Journal of Pharmaceutical Sciences,* pp. 70-74.

RXList, 2017. *Rosuvastatin Calcium.* [Online]
Available at: https://www.rxlist.com/rosuvastatin-calcium-drug.htm

Rzepczynska, I. et al., 2009. Role of isoprenylation in simvastatin-induced inhibition of ovarian theca-interstitial growth in the rat. *Biological Reproduction,* pp. 850-855.

Sacks, F. et al., 1996. The effect of pravastatin on coronary events after myocardial infarction in patients with average cholesterol levels.. *New England Journal of Medicine,* pp. 1001-1009.

Sánchez-Quesada, J., Otal-Entraigas, C. & Franco, M., 1999. Effect of simvastatin treatment on the electronegative low-density lipoprotein present in patients with heterozygous familial hypercholesterolemia. *American Journal of Cardiology,* pp. 655-659.

Sanchis-Gomar, F., Perez-Quilis, C., Leischik, R. & Lucia, A., 2016. Epidemiology of coronary heart disease and acute coronary syndrome. *Annals of translational medicine.*

Scandinavian Simvastatin Survival Study Group, 1994. Randomised trial of cholesterol lowering in 4444 patients with coronary heart disease: the Scandinavian Simvastatin Survival Study (4S). *The Lancet,* pp. 1383-1389.

Schachter, M., 2005. Chemical, pharmacokinetic and pharmacodynamic properties of statins: an update. *Fundamental & clinical pharmacology,* pp. 117-125.

Schwartz, G. et al., 2001. Myocardial Ischemia Reduction with Aggressive Cholesterol Lowering (MIRACL) Study Investigators. Effects of atorvastatin on early recurrent ischemic events in acute coronary syndromes: the MIRACL study: a randomized controlled trial. *JAMA,* pp. 1711-1718.

Serruys, P. et al., 2002. Fluvastatin for prevention of cardiac events following successful first percutaneous coronary intervention: a randomized controlled trial. *Jama,* pp. 3215-3222.

Sever, P. et al., 2005. Reduction in cardiovascular events with atorvastatin in 2,532 patients with type 2 diabetes: Anglo-Scandinavian Cardiac Outcomes Trial–lipid-lowering arm (ASCOT-LLA). *Diabetes care,* pp. 1151-1157.

Shah, T. V. & Vasava, D. V., 2019. A glimpse of biodegradable polymers and their biomedical applications. *e-Polymers,* 19(1).

Shepherd, J. et al., 1995. Prevention of coronary heart disease with pravastatin in men with hypercholesterolemia. *New England Journal of Medicine,* pp. 1301-1308.

Stapleton, F. et al., 2006. Silicone Hydrogel Contact Lenses and the Ocular Surface. *The Ocular Surface,* 4(1), pp. 24-43.

Subramanian, S. et al., 2013. High-dose atorvastatin reduces periodontal inflammation: a novel pleiotropic effect of statins. *Journal of the American College of Cardiology,* p. 2382–2391.

Sun, B. et al., 2018. Comparative analysis of the gut microbiota in distinct statin response patients in East China. *Journal of Microbiology,* pp. 886-892.

Sweilam, N., Khader, M. M. & Mahdy, M. S., 2012. Crank-Nicholson Finite Difference Method For Solving Time-Fractional Diffusion Equation. *Journal of Fractional Calculus and Applications,* 2(Jan), pp. 1-9.

U.S. Department of Health and Human Services, 2013. *Bioequivalence Studies with Pharmacokinetic Endpoints for Drugs Submitted Under an ANDA.* [Online] Available at: https://www.fda.gov/files/drugs/published/Bioequivalence-Studies-With-Pharmacokinetic-Endpoints-for-Drugs-Submitted-Under-an-Abbreviated-New-Drug-Application.pdf

U.S. Food and Drug Administration, 2005. *CRESTOR.* [Online]
Available at:
https://www.accessdata.fda.gov/drugsatfda_docs/label/2005/21366slr005lbl.pdf

Walter, J., 2008. Ecological role of lactobacilli in the gastrointestinal tract: implications for fundamental and biomedical research. *Applied and environmental microbiology,* pp. 4985-4996.

Wang, L. et al., 2018. The influence of the intestinal microflora to the efficacy of Rosuvastatin. *Lipids in health and disease,* p. 151.

Witztum, J. & Steinberg, D., 2001. The oxidative modification hypothesis of atherosclerosis: does it hold for humans?. *Trends in Cardiovascular Medicine,* pp. 93-102.

Wu, H. et al., 2017. Rosuvastatin pharmacokinetics in Asian and white subjects wild type for both OATP1B1 and BCRP under control and inhibited conditions. *Journal of pharmaceutical sciences,* pp. 2751-2757.

Yatsunenko, T. et al., 2012. Human gut microbiome viewed across age and geography. *Nature,* pp. 222-227.

Zhao, Y., Wu, T., Zhao, M. & Li, C., 2020. The balance of protein farnesylation and geranylgeranylation during the progression of nonalcoholic fatty liver disease. *Journal of Biological Chemistry,* pp. 5152-5162.

Zhou, Q. & Liao, J., 2009. Statins and cardiovascular diseases: From cholesterol lowering to pleiotropy.. *Current Pharmaceutical Design,* pp. 467-478.

Zhou, Q. & Liao, J., 2009. tatins and cardiovascular diseases: from cholesterol lowering to pleiotropy.. *Current pharmaceutical design,* 15(5), pp. 467-478.

Zhou, W. et al., 2020. Implication of Gut Microbiota in Cardiovascular Diseases. *Oxidative Medicine and Cellular Longevity.*